

Review

## Modeling electrostatic effects in proteins

Arieh Warshel<sup>a,\*</sup>, Pankaz K. Sharma<sup>a</sup>, Mitsunori Kato<sup>a</sup>, William W. Parson<sup>b</sup>

<sup>a</sup> University of Southern California, 418 SGM Building, 3620 McClintock Avenue, Los Angeles, CA 90089-1062, USA

<sup>b</sup> Department of Biochemistry, Box 357350, University of Washington, Seattle, WA 98195-7350, USA

Received 2 May 2006; received in revised form 17 August 2006; accepted 18 August 2006

Available online 25 August 2006

### Abstract

Electrostatic energies provide what is perhaps the most effective tool for structure–function correlation of biological molecules. This review considers the current state of simulations of electrostatic energies in macromolecules as well as the early developments of this field. We focus on the relationship between microscopic and macroscopic models, considering the convergence problems of the microscopic models and the fact that the dielectric ‘constants’ in semimacroscopic models depend on the definition and the specific treatment. The advances and the challenges in the field are illustrated considering a wide range of functional properties including  $pK_a$ 's, redox potentials, ion and proton channels, enzyme catalysis, ligand binding and protein stability. We conclude by pointing out that, despite the current problems and the significant misunderstandings in the field, there is an overall progress that should lead eventually to quantitative descriptions of electrostatic effects in proteins and thus to quantitative descriptions of the function of proteins.

© 2006 Elsevier B.V. All rights reserved.

**Keywords:** Electrostatic effect; Enzyme catalysis; Ion channel; Proton channel; Generalized Born model; Macroscopic model; PDL/S-LRA; Convergence; Long-range effect; Helix dipole; Computer modeling;  $pK_a$

### 1. Introduction

Electrostatic effects play major roles in proteins [1–3], and the ability to quantify electrostatic interactions is essential for any structure–function correlation in proteins. Accomplishing this task, however, is far from simple. The foundation of the classical theory of continuum electrostatics was laid in the eighteenth century with the landmark work of Charles Augustin Coulomb, which was later, in the nineteenth century, formulated rigorously by James Clark Maxwell. However, this formal progress and the analytical solutions that were obtained for a few simple cases did not provide adequate tools for calculating electrostatic energies in proteins. Here one faced electrostatic interactions at microscopically small distances where the concept of a dielectric constant is problematic, and the irregular shape of protein environments made the use of analytical models impractical. Nevertheless, the realization that some aspects of protein action must involve electrostatic interactions

led to the emergence of simplified macroscopic models [4,5] that could provide useful insights [3,6,7].

The availability of X-ray and NMR structures of many proteins, coupled with the search for a more quantitative theoretical understanding of protein structure and function, led to the emergence of microscopically based studies of electrostatic effects in proteins [8–11]. These studies and subsequent numerical continuum studies led to the gradual realization that electrostatic energies provide by far the best structure–function correlator for proteins and other macromolecules. Yet the appeal of macroscopic concepts such as the dielectric constant still leads to widespread confusion about the strengths and limitations of various approaches to calculating electrostatic energies.

This review will consider microscopic, macroscopic and semimacroscopic calculations of electrostatic effects in proteins. We will try to lead the reader from concepts to models and applications, pointing out some of the pitfalls and promising directions. Additional background material and varying perspectives on the topic can be found in several other reviews [3,6–9,12–15].

\* Corresponding author. Tel.: +1 213 740 4114; fax: +1 213 740 2701.

E-mail address: [warshel@usc.edu](mailto:warshel@usc.edu) (A. Warshel).

## 2. The emergence of electrostatic modeling of proteins

All electrostatic theories start basically from the experimental observations that led to Coulomb's law, which expresses the free energy (the reversible work) of bringing two charges ( $Q_i$  and  $Q_j$ ) together in a vacuum by

$$\Delta G = 332Q_iQ_j/r_{ij}. \quad (1)$$

Here the free energy ( $\Delta G$ ) is given in kcal/mol, the distance ( $r_{ij}$ ) in Å, and the charges in atomic units. Manipulations of Eq. (1) lead to the general macroscopic equation for the macroscopic electric field ( $\mathbf{E}$ ) [16]:

$$\mathbf{E}(\mathbf{r}) = \int \frac{(\mathbf{r} - \mathbf{r}')\rho(\mathbf{r}')}{|\mathbf{r} - \mathbf{r}'|^3(\mathbf{r} - \mathbf{r}')^2} d\mathbf{r}', \quad (2)$$

where  $\rho$  is the charge density ( $\rho(\mathbf{r}) = \sum_i Q_i \delta(\mathbf{r} - \mathbf{r}_i)$ ). The field  $\mathbf{E}$  also can be expressed as the gradient ( $\nabla = (\mathbf{i}\partial/\partial x, \mathbf{j}\partial/\partial y, \mathbf{k}\partial/\partial z)$ ) of a scalar potential,  $U$ :

$$\mathbf{E}(\mathbf{r}) = -\nabla U(\mathbf{r}) \quad (3)$$

it is also important to keep in mind that the above macroscopic field can be obtained by averaging the field due to the microscopic dipoles (plus any external field) in a macroscopically small region (see Ref. [12] for discussion).

Further manipulation of Eqs. (1) and (2) leads to the Poisson equation:

$$\nabla^2 U(\mathbf{r}) = -4\pi\rho(\mathbf{r}) \quad (4)$$

where  $\nabla^2 = \partial^2/\partial x^2 + \partial^2/\partial y^2 + \partial^2/\partial z^2$ . For a condensed medium in which dielectric effects can be represented by a dielectric constant,  $\varepsilon(\mathbf{r})$ , Eq. (4) becomes

$$\nabla[\varepsilon(\mathbf{r})\nabla U(\mathbf{r})] = -4\pi\rho(\mathbf{r}) \quad (5)$$

if ions are present in the solution and are distributed according to a Boltzmann distribution we obtain, for weak fields, the linearized Poisson–Boltzmann (PB) equation:

$$\nabla[\varepsilon(\mathbf{r})\nabla U(\mathbf{r})] = -4\pi\rho(\mathbf{r}) + \kappa^2 U(\mathbf{r}), \quad (6)$$

where  $\kappa^2$  is the Debye–Hückel screening parameter.

The problem with these seemingly rigorous expressions is the weakness of their physical foundation. Not only are the continuum assumptions problematic on a molecular level, but also the nature of the dielectric constant in Eq. (5) is unclear when applied to heterogeneous environments. Despite this obvious difficulty, early studies of electrostatics effects in proteins were dominated by phenomenological models that used a uniform dielectric constant for protein interiors. Perhaps the most influential such model was the Tanford–Kirkwood (TK) model [5], which described the protein as a sphere with a uniform and low dielectric constant.

Although the TK model helped to inspire other early studies of electrostatic interactions in proteins, it reflected assumptions that were formulated before much was known about actual protein structures. For example, Tanford and Kirkwood assumed

that all the ionized groups are located on the protein surface, which has turned out to be incorrect in many cases. Subsequent analysis by Warshel and coworkers [10] indicated that the TK model also ignored one of the most important physical aspects of protein electrostatics, the self-energy of a charged group (the energy of charging the group in its protein site when all the other ionizable groups are neutral). Nevertheless, the TK model is still often invoked as a physically reasonable model, with only the assumption of a spherical shape being regarded as a rough approximation.

The work of Warshel and Levitt [11], which marked the emergence of modern studies of electrostatic effects in proteins, started from the realization that the only way to reach unique conclusions about the energetics of enzyme catalysis was to abandon the concept of a dielectric constant and to develop a simplified microscopic model that included all the significant contributions. The solvent was modeled by using an explicit grid of Langevin dipoles (LD) and the protein also was modeled explicitly, taking into account its permanent and induced dipoles. Reorganization of the protein structure around charged groups was treated in a limited way by energy minimization. The resulting Protein–Dipoles–Langevin–Dipoles (PDL) model was the first model to capture correctly the physics of protein electrostatics, and the basic microscopic perspective of this model continues to provide the best way of avoiding the traps of continuum concepts.

Poisson–Boltzmann (PB) models [3,17,18] solve Eq. (6) or its nonlinear extension for stronger fields by using a finite difference grid and treating the shape of the protein in detail, while continuing to use macroscopic dielectric constants for both the protein and the solvent. This approach has been widely accepted, in part because of its relative simplicity, but perhaps also because of the lingering impact of the seemingly authoritative continuum Equations (Eqs. (2)–(6)). Early PB models used unjustified dielectric constants (see for discussion, Refs. [12,19]) and ignored some of the major conceptual problems that can be resolved by using microscopic models [8,10,12,20], including the self-energies of charged groups and the effects of the protein's permanent dipoles [10]. However, these macroscopic models have evolved into more microscopic forms and in many respects have converged to the PDL model and its semi-macroscopic version, the PDL/S-LRA model (see below).

Although we now have a wide range of reasonable electrostatic models, there still appear to be major misunderstandings about some aspects of these models. Some of these issues will be addressed in Sections 3 and 4. As we will discuss, almost any conceptual problem of a continuum model can be resolved and clarified by the use of microscopic concepts. Perhaps the best example is the elucidation of the nature of the protein dielectric constant [12,19], which we discuss in Section 4.

Early, insightful observations by Perutz [1] and others [21–23] indicated that electrostatic interactions play an important role in biology. However, it was the development of computational methods for assessing these interactions reliably that led to recognition of the power of using calculated electrostatic

energies for structure–function correlation for proteins [2]. This has been demonstrated in studies of a wide range of properties that will be considered in Sections 6–15.

### 3. The hierarchy of electrostatic models

Studies of electrostatic effects in proteins have involved a wide range of modeling approaches that can be roughly divided into microscopic all-atom models, simplified dipolar models, and macroscopic models (see Fig. 1). Microscopic models can be divided further into classical and quantum mechanical treatments. Each of these models has its own scope and limitations. This includes, of course, the difficulty of interpreting continuum results without the use of microscopic models. Thus, it is important to understand the relationships between various approaches.

#### 3.1. All-atom models, boundary conditions, long-range treatments, polarizability effects and convergence

An all-atom model describes a system as a collection of particles that interact via a quantum mechanical potential surface that can be approximated by a proper empirical force field. Although such approaches can be quite rigorous, adequate convergence may sometimes not be achieved even with nanosecond simulations, particularly for macromolecules. One of the most significant “unresolved” issues in atomistic simulations is the proper representation of an infinite system, which is critical for a proper treatment of long-range electrostatic effects. Periodic boundary conditions (e.g., [24]), although appropriate in non-polar systems for non-electrostatic problems or in periodic molecular crystals, cannot produce truly infinite non-crystalline systems without artifacts when long-range electrostatic interactions are significant (e.g., see Fig. 5 in Ref. [25]). It is only now becoming commonly appreciated that the Ewald method for periodic boundary conditions gives divergent solvation energies for the same solute depending on the size of the simulated system (e.g., [26]). Correction formulas for particular charge distributions [27] do not provide a general solution (see discussion in [28] and [29]). In fact, Refs. [29–32] demonstrated that the Ewald PME method, which has become more or less a standard tool in molecular simulations, provides inadequate treatment of electrostatic energies for non-periodic systems. The same is true for Ewald treatments with tin-foil boundaries and atom-based cutoffs. As demonstrated elsewhere (e.g., [32–34]), this problem, which was anticipated long ago (e.g., [25,35]), does not occur in simulations that use spherical boundary conditions and utilize the local reaction field (LRF) approach [36]. Spherical boundary conditions including a spherical Ewald-type model [35] are physically more consistent than the periodic Ewald methods because there is no spurious periodicity; a spherical region of atomic representation is just surrounded by a region that is treated more simply. Because the simplified outer region is far from the focal point of the simulation, its effect can be made indistinguishable from that of an atomistic representation.

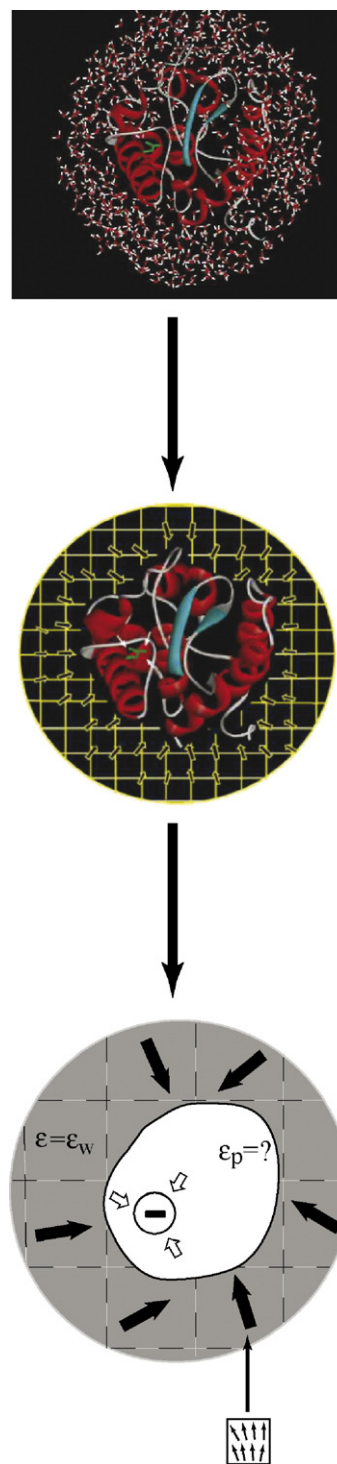


Fig. 1. The three main options for representing the solvent in computer simulation approaches. The microscopic model uses a detailed all-atom representation and evaluates the average interaction between the solvent residual charges and the solute charges. Such calculations are comparatively slow and expensive. The simplified microscopic model replaces the time average dipole of each solvent molecule by a point dipole, while the macroscopic model uses a polarization vector to represent a collection of solvent dipoles in a large volume element.

The issues involved in constructing proper boundaries for spherical models are logical and obvious. The most important requirement is that the system maintains proper polarization at

and around the boundaries [37]. This requirement is, in the case of polar systems, much more important than the physically trivial requirement of maintaining proper heat flow by stochastic boundaries [38,39] and has been achieved by the surface constraint all-atom solvent (SCAAS) model [40]. The problem is not the well-known bulk contribution from the surroundings of the simulation sphere [41], which can be implemented easily in simulation studies [42,43], but the polarization at the microscopic boundaries of the simulation sphere [40].

Another important issue is the inclusion of the effect of induced dipoles in microscopic simulations of electrostatic energies. The use of polarization terms in force fields dates back to the work of Warshel and Levitt, who introduced this approach as general way of capturing the effect of the electronic polarization in protein modeling. This was done by both iterative and non-iterative approaches. The use of a polarizable force field became an integral part of simulations in the Warshel group [42,44], who analyzed its effect on electrostatic modeling in many studies [12,45,46]. The general realization that the effects of induced dipoles are quite important has been quite slow (some workers initially argued that these effects could not be significant [47]), but is now widely appreciated. Several groups have started to develop different types of polarizable force fields [48,49], which is clearly an important and overdue step. However, it is important to realize (in contrast to the possible impression given by some of these recent works) that the use of polarizable force fields is not a new development and that there is already a significant body of knowledge on cases where the effects of induced dipoles are important, and also on other cases where such a treatment is not crucial.

With reasonable boundary conditions, proper long-range treatment and induced dipoles, one can use all-atom models for evaluation of electrostatic free energies. The most appropriate approach usually is the free energy perturbation (FEP) method [50,51]. This approach involves gradually changing the solute charge from zero to its actual value  $Q=Q_0$  using a series of mapping potentials of the form

$$V_m = (1 - \lambda_m)V(Q=0) + \lambda_m V(Q_0), \quad (7)$$

where  $\lambda_m$  is changed gradually from 0 to 1 [50,52]. The corresponding free energy change then is evaluated by the expression

$$\exp\{-\Delta G(\lambda_m \rightarrow \lambda_{m+1})\beta\} = \langle \exp\{-(V_{m+1} - V_m)\beta\} \rangle_{V_m}, \quad (8)$$

where  $\langle \rangle_{V_m}$  designates a molecular dynamics (MD) average over  $V_m$  and  $\beta=1/k_B T$ . The overall charging free energy is obtained by collecting the  $\Delta G(\lambda_m \rightarrow \lambda_{m+1})$ . A very useful alternative is to use the linear response approximation (LRA), in which the free energy is given by [53]

$$\Delta G(Q=0 \rightarrow Q=Q_0) = \frac{1}{2} \left[ \langle V(Q_0) - V(Q=0) \rangle_{V(Q_0)} + \langle V(Q_0) - V(Q=0) \rangle_{V(Q=0)} \right]. \quad (9)$$

Although the FEP and LRA approaches are both fundamentally sound, they can involve major convergence problems when

applied to charges in proteins, and they have been explored systematically in only a relatively small number of studies (e.g., [50,54,55]).

Another seemingly rigorous approach for studies of electrostatic energies in proteins and, in particular, for studying the free energy profile of ions in ion channels, is to evaluate the so-called potential of mean force (PMF). The PMF reflects the free energy of moving a given charged group from the bulk solvent to a specific protein site, and is typically evaluated by using umbrella sampling (US) or related approaches [52,57]. In the PMF approach, one commonly uses a mapping potential of the form

$$\varepsilon_m = (1 - \lambda_m)\varepsilon_1 + \lambda_m\varepsilon_2 \quad (10a)$$

$$\varepsilon_1(z) = E_g(z) + K(z - z_0^{(1)})^2 = E_g(z) + E_{\text{cons}}^{(1)} \quad (10b)$$

$$\varepsilon_2(z) = E_g(z) + K(z - z_0^{(2)})^2 = E_g(z) + E_{\text{cons}}^{(2)}. \quad (10c)$$

Here  $z_0^{(1)}$  and  $z_0^{(2)}$  are neighboring points on a reaction coordinate ( $z$ ) such as the position of solvated  $\text{Na}^+$  ion in a transmembrane channel,  $K$  is a quadratic constraint that holds the system at a specified point, and  $E_g(z)$  is the total potential of the system without the constraints. The free energy then can be obtained by the FEP/US formula [57]

$$\Delta g(z) = -\frac{1}{\beta} \ln \left[ \exp\{-\Delta G(\lambda_m)\beta\} \langle \delta(z' - z) \exp\{E_{m,\text{cons}}(z)\beta\} \rangle_{\varepsilon_m} \right]. \quad (11)$$

where,  $\Delta G(\lambda_m)$  is the FEP energy associated with the change of  $\lambda$  from zero to  $\lambda_m$ , and  $E_{m,\text{cons}}(z)$  is  $E_g - E_m$ .

Some workers replace the  $\Delta G(\lambda_m)$  term in Eq. (11) by a term obtained by the “weighted histograms analysis method” (WHAM), which is intended to provide the best overlap of results from simulations at different  $z'$  [58]. In our experience, the WHAM approach does not improve the results [57]. This is worth noting, since the presumed advantages of the WHAM approach and the seemingly rigorous formulation of PMF methods (and related approaches such as Jarzynski’s formula [59]) have drawn attention from the main question, which is whether the PMF approach can provide reliable electrostatic energies. Few of the benchmarks in PMF studies have considered well-defined electrostatic problems that test the method critically; most have considered less relevant systems, such as the alanine dipeptide [60,61]. In fact, PMF approaches suffer from major hysteresis problems, and suffer from the enormous challenge of calculating the reversible work of moving the ion from the bulk solvent to the protein interior. Furthermore, since PMF approaches do not provide absolute solvation free energies, they generally do not give a clear warning about major problems with the simulation method used or with the specific treatment of long-range effects.

Although PMF calculations will be discussed further in Sections 5, 7 and 14, it is pertinent to mention here a recent study [57] in which we compared FEP-based PMF to the adiabatic charging (AC) approach, a non-standard PMF method that involves pulling the ion using Eqs. (10) and (11). The comparison was done for a well-defined benchmark composed of a

small part from the gramicidin A channel with various degrees of solvation. The results, summarized in Fig. 2, indicate that the PMF approach converges to the AC results only very slowly.

### 3.2. The LD and PDL models are simplified, thermally averaged microscopic models

The most natural simplification of all-atom polar models is to represent molecules or groups of atoms as dipoles. This picture has a long history in the theory of polar solvents, and it was used as a conceptual starting point in the development of electrostatic theories [62]. Simulations with “sticky” dipoles [63] and formal studies [64] addressing the origin of the dipolar representation have been described. The nature of the Brownian dipole lattice (BDL) and Langevin dipole (LD) models and their relationship to continuum models have been established [65]. This study indicated that continuum solvation models are the infinite dipole density limit of a more general dipolar representation, and that their linearity is a natural consequence of being at that limit (although the discreteness of dipole lattice models is not equal to that of continuum models [66]). It also was found that the solvation behavior of the LD model is identical to that of the more

rigorous BDL model. This is significant since, as mentioned above, a version of the LD model, the protein dipoles Langevin dipoles (PDL) model, has been used extensively to treat electrostatics in macromolecules [12].

The PDL model has been criticized by some workers who appear to consider even macroscopic models as more realistic descriptions of macromolecules. These criticisms have reflected major misunderstandings that have been addressed elsewhere (see footnote 21 in [54]), and the logic of some of the early criticisms seems hard to follow today (see, e.g. [67]). An example is the statement [68] that the PDL model of reference [11] does not evaluate self-energies, and the assertion that this model is, in fact, macroscopic in nature and is physically equivalent to using a finite-difference grid in PB or any other discretized continuum (DC) methods. These assertions involve a misunderstanding of the physics of dipolar solvents. The grid of dipoles with a finite spacing used in the PDL model, or the equivalent system of polar molecules on a lattice, is not at all equivalent to the numerical grid used in evaluating the electrostatic potential in DC approaches (see footnote 26 in [54]). However, Simonson [9] recently has repeated the incorrect claim that the LD and DC models are equivalent. He remarks that “The LD model is not only analogous to the continuum model (as stated many times in the literature), but identical to the continuum model in its discrete approximation,” continuing “to our knowledge this rigorous equivalence was only pointed out very recently [69]”. These statements reflect a misunderstanding of the conclusions of the careful study by Borgis and coworkers [69]. They also overlook rigorous studies of dipolar lattices [66], which showed that the LD and DC models have different structural features even at the limit of infinitely small spacing.

In view of the above confusion, it is important to note that, in spite of its simplicity, the LD model (with its finite spacing of Langevin dipoles) has always been a fully microscopic model. The clear physical features of the model (i.e., the interpretation of each grid point as a discrete particle with a dipole that depends on the field at that point) has prevented the PDL model from falling into the traps that beset continuum models of proteins. For example, focusing on the microscopic interactions of charged groups with their surroundings led immediately to an explicit treatment of the protein’s permanent dipoles, rather than a problematic attempt to represent these dipoles by a low dielectric constant. Saying that the LD model (or any other dipolar model) is equal to a continuum model thus is similar to saying that an all-atom model is the same as a continuum model. If the reader is still confused by the suggestion that the LD model is a continuum model [9,68], it may help to point out that, whereas macroscopic models involve scaling electrostatic energies by a dielectric constant, no such scaling is used in the PDL model.

### 3.3. The PDL/S-LRA model provides a consistent semi-microscopic treatment

Microscopic models that evaluate the absolute electrostatic energy (including the PDL model) do not involve a

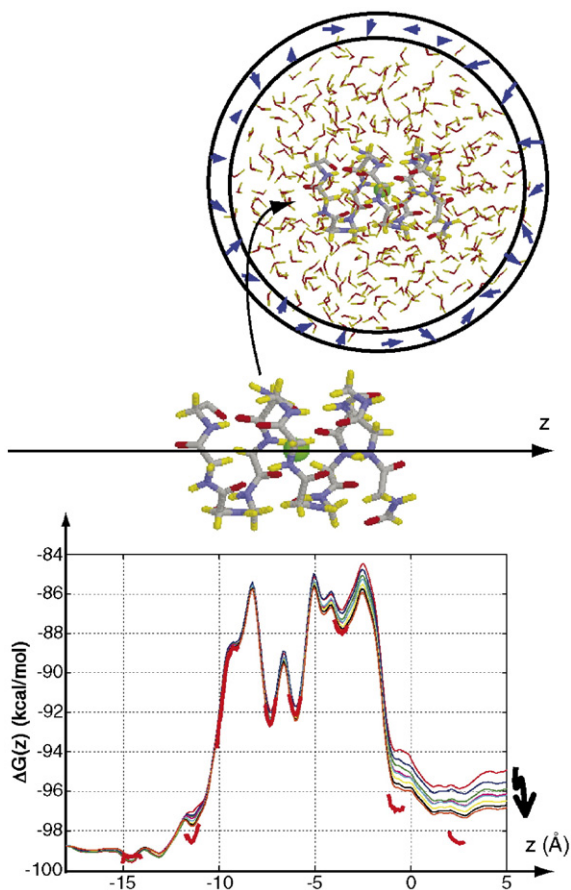


Fig. 2. Comparison of PMF and adiabatic-charging (AC) results for moving  $\text{Na}^+$  through the gramicidin A channel. The figure shows the AC results (red dashed line) for 130 ns and PMF results (thin, colored lines) for simulations of 140, 280, 420, 560, 700, 840 and 980 ns and 1.12  $\mu\text{s}$ . The PMF results converge very slowly to the AC results. Adapted from [57].

dielectric constant; induced dipoles in the protein and solvent are evaluated explicitly. This provides a rigorous formulation, but is sometimes a practical “weakness” since it involves the balance between large, opposing contributions, which can be difficult to obtain in the absence of perfect convergence. Because the balance must exist, in some cases it can be represented adequately by scaling the calculated energies with a dielectric constant (see Section 4). Such a philosophy leads to semi-macroscopic models that are more stable (but not necessarily more reliable) than the corresponding microscopic models. A practical way of exploiting the stability of the semi-macroscopic models, while keeping a clear physical picture, is the semi-macroscopic version of the PDL model (PDL/S) [70]. The PDL/S model starts with the PDL model and then scales the corresponding contributions by assuming that the protein has a dielectric constant  $\epsilon_p$ . To reduce the unknown factors in  $\epsilon_p$  it is useful to transform the PDL/S model to the PDL/S-LRA model. In this treatment, the PDL/S energy is evaluated within the LRA approximation and is averaged over configurations generated by MD simulations of the charged and the uncharged states [19,42,54]. The MD simulations generate protein configurations automatically for the charged and uncharged forms of the system, and the contributions of the different configurations are averaged according to Eq. (9). The PDL/S treatment expresses the free energy of moving a single charge from water to the protein active site as:

$$\Delta\Delta G_{\text{sol}}^{w\rightarrow p} = \frac{1}{2} \left[ \langle \Delta U^{w\rightarrow p} \rangle_{Q_0} + \langle \Delta U^{w\rightarrow p} \rangle_{Q=0} \right], \quad (12)$$

where,

$$\Delta U^{w\rightarrow p} = \left[ \Delta\Delta G_p^w(Q=0 \rightarrow Q=Q_0) - \Delta G_Q^w \right] \left( \frac{1}{\epsilon_p} - \frac{1}{\epsilon_w} \right) + \Delta U_{Q\mu}^p(Q=Q_0) \frac{1}{\epsilon_p}. \quad (13)$$

Here  $\Delta G_g^w$  is the solvation energy of the charge in water,  $\Delta\Delta G_p^w$  is the change in the solvation energy of the entire protein (including the bound charge) upon changing this charge from zero to its actual value ( $Q_0$ ).  $\Delta U_{Q\mu}^p$  is the microscopic electrostatic interaction of the charge with the surrounding protein polar groups. For simplicity, we assume here that the interaction with the protein ionizable groups is treated in a separate cycle [54].

Eq. (13) probably provides the clearest connection between semimacroscopic treatments and microscopic quantities such as  $\Delta\Delta G_p^w$  and  $\Delta U_{Q\mu}^p$ . The PDL/S treatment without the LRA treatment converges to the Poisson–Boltzmann (PB) treatment, providing a useful connection between PB treatments and microscopic treatments and clarifying the exact nature of  $\epsilon_p$  (see [19] and Section 4). By using Eq. (12) to treat the protein reorganization explicitly, the LRA reduces the uncertainties in the magnitude of  $\epsilon_p$ . The molecular mechanics PB surface area (MM-PBSA) model [71] adopts the PDL/S-LRA idea of using MD to generate configurations for implicit solvent

calculations, but calculates only the average over the configurations generated with the charged solute (the first term in Eq. (9), rather than the fully consistent LRA expression).

### 3.4. Macroscopic continuum models depend critically on the assumed $\epsilon_p$

As mentioned in Section 2, early macroscopic continuum models such as the Tanford–Kirkwood model [5] and early discretized-continuum (DC), or Poisson–Boltzmann (PB) models [18,72,73] treated the protein as a uniform dielectric medium without considering the effect of the protein’s permanent dipoles ( $\Delta U_{Q\mu}^p$  in Eq. (13)). The TK model [5] also omitted the self-energy term (see discussion in [10,74]). More recent PB models resemble the PDL model in including the protein permanent dipoles explicitly, while using a macroscopic-continuum approach to treat dielectric effects [3,75–90]. These models, as implemented in the programs DelPhi [75,77,91], UHBDP [92] and APBS [93], map the protein–solvent system to a cubic grid with two dielectric regions. The region representing the solvent usually is assigned a macroscopic dielectric constant similar to that of water ( $\epsilon_s \approx 80$ ), while that representing the protein is given a lower dielectric constant ( $\epsilon_p$ ) between 2 and 40. The electric potential  $U(\mathbf{r})$  at each grid point is evaluated by solving the Poisson–Boltzmann equation subject to the boundary condition that the potential goes to the value given by the Debye–Hückel theory at long distances from the protein. As stated above, the nature of the PB results can be best analyzed by using the PDL/S formulation. With this in mind, the electrostatic energy of a single charge,  $Q$ , in processes such as reduction or protonation can be written as,

$$G_{\text{elec}} = \Delta U_{Q\mu}^p / \epsilon_p + G_{\text{RF}}, \quad (14)$$

where,  $\Delta U_{Q\mu}^p$  is again given by Eq. (13) and  $G_{\text{RF}}$  (the “reaction field” energy) represents interactions of the protein charges with the fields from the solvent and electrolytes. Some recent implementations of the PB model also include sampling of multiple protonation states and rotational conformers of polar hydrogens [81,83,85,87], which in many respects resembles the more rigorous LRA treatment in the PDL/S-LRA model described above.

Regardless of the above developments, it appears to us that the popularity of PB models stems partly from the erroneous belief that the PB equation reflects fundamental physics, so that any criticisms of it must concern only matters of implementation that could be fixed in one way or another. The discussion of conceptually trivial technical issues such as the linear approximation of the second term in Eq. (6) may create the impression that these issues are the main drawback of such models. In fact, the real problem is that the results depend critically on  $\epsilon_p$ , whose value cannot be determined uniquely (see Section 4). The wide acceptance of PB models also may rest partly on insufficiently critical validations, most of which have used trivial cases of surface groups where all macroscopic models would give essentially the same results (see Section 5).

### 3.5. The generalized born model is basically equivalent to coulomb's law with a distance-dependent dielectric constant

In treating electrostatic energies in macromolecules it is convenient to use a two-step thermodynamic cycle. The first step involves transfer of each ionized group from water to its site in the protein with all other groups neutral; interactions between the ionized groups are turned on in the second step [19]. Using this cycle, we can write the energy of moving ionized groups from water to their protein site as,

$$\Delta G = \sum_{i=1}^N \Delta G_i + \sum_{i>j} \Delta G_{ij}, \quad (15)$$

where the first and second terms correspond to the first and second steps, respectively.  $\Delta G_i$ , which represents the change in self-energies of the  $i$ th ionized group upon transfer from water to the protein site, can be evaluated by the PDL/D/S-LRA approach with a relatively small  $\epsilon_p$ . However, the charge–charge interaction terms (the  $\Delta G_{ij}$ ) are best reproduced by using a simple macroscopic Coulomb's-type law and by expressing the overall electrostatic energy as

$$G_{\text{elec}} = G_{\text{sol}}^{\infty} + 332 \sum_{i=1}^{n-1} \sum_{j=i+1}^n Q_i Q_j / r_{ij} \epsilon_{\text{eff}}^{ij}, \quad (16)$$

where  $G_{\text{sol}}^{\infty}$  is the sum of the solvation free energies (in kcal/mol) of the individual charges at infinite separation in the simple case of homogeneous medium,  $r$  again is in Å, and  $\epsilon_{\text{eff}}^{ij}$  is an empirical, distance-dependent dielectric screening factor [10]. Several general forms have been used for  $\epsilon_{\text{eff}}^{ij}$ , including the simple exponential function,

$$\epsilon_{\text{eff}}(r_{ij}) = 1 + \epsilon' [1 - \exp(-\mu r_{ij})], \quad (17)$$

where  $\epsilon' \approx 60$  and  $\mu$  is in the range of 0.1 to 0.2 Å<sup>-1</sup> [10,12]. Sigmoidal functions that give similar screening at distances greater than 10 Å also have been used [94–98].

Eq. (17) with either an exponential or sigmoidal screening function was found to reproduce the effects of mutations of ionizable residues on the  $E_m$  of P/P<sup>+</sup>, the reactive bacteriochlorophyll dimer in bacterial reaction centers [99]. The simple linear scaling,  $\epsilon_{\text{eff}}^{ij} = r_{ij}$ , increases more slowly with distance, and did not work well in that case.

Although the fact that protein groups separated by more than about 10 Å are screened by a large factor ( $\epsilon_{\text{eff}}^{ij} \geq 40$ ) is supported by numerous mutation experiments (e.g., [45,99]) and conceptual considerations [12], many workers in the field apparently still consider the use of Eqs. ((15)–(17)) to be poor approximations in comparison to PB treatments. We see no basis for this view, considering that the PB approach depends entirely on an unknown  $\epsilon_p$  (see below).

The so-called generalized Born (GB) model [68,100–111], whose usefulness is now widely appreciated, is basically a version of Eq. (16). The GB approach can be developed by noting that the electrostatic free energy of a set of charges in an infinite homogeneous medium with dielectric constant  $\epsilon_{\text{eff}}$  can

be written as the sum of the gas-phase energy ( $\Delta U_{\text{QQ}}$ ) and the solvation free energy ( $G_{\text{sol}}$ ):

$$G_{\text{elec}} = \Delta U_{\text{QQ}} + G_{\text{sol}} \quad (18)$$

$$\Delta U_{\text{QQ}} = 332 Q_i Q_j / r_{ij}$$

Alternatively, the electrostatic free energy can be expressed as the sum of the solvation free energies of the individual charges at infinite separation ( $G_{\text{sol}}^{\infty}$ ) plus the free energy of bringing the charges in from infinity to their actual positions ( $\Delta U_{\text{QQ}}/\epsilon_{\text{eff}}$ ):

$$G_{\text{elec}} = G_{\text{sol}}^{\infty} + \Delta U_{\text{QQ}}/\epsilon_{\text{eff}}. \quad (19)$$

The solvation free energy of an individual charge ( $Q_i$ ) at infinite separation can be related to the solvation free energy of a charged sphere of radius,  $a_i$  (the “Born radius”), embedded in an infinite medium of dielectric constant  $\epsilon_{\text{eff}}$ , through the relationship

$$G_{\text{sol}(i)}^{\infty} = -332(1 - 1/\epsilon_{\text{eff}})(Q_i^2/2a_i) \quad (20)$$

[112]. Combining Eqs. (18)–(20) and summing the individual Born energies, we have

$$G_{\text{sol}} = G_{\text{sol}}^{\infty} - \Delta U_{\text{QQ}}(1 - 1/\epsilon_{\text{eff}}) \quad (21a)$$

$$= -332 \left\{ \sum_{i=1}^n (Q_i^2/2a_i) + \sum_{i=1}^{n-1} \sum_{j=i+1}^n (Q_i Q_j / r_{ij}) \right\} \times (1 - 1/\epsilon_{\text{eff}}). \quad (21b)$$

In GB treatments, the sums in Eq. (21b) are combined further by writing

$$G_{\text{sol}}^{\text{GB}} = -166 \left( 1 - \frac{1}{\epsilon_{\text{eff}}} \right) \sum_{i=1}^n \sum_{j=1}^n \frac{Q_i Q_j}{f_{ij}}, \quad (22)$$

where  $f_{ij}$  is an empirical function of distance. A commonly used function is

$$f_{ij} = [r_{ij}^2 + a_i a_j \exp(-r_{ij}^2/4a_i a_j)]^{1/2}, \quad (23)$$

where  $a_i$  and  $a_j$  are “effective” Born radii for atoms  $i$  and  $j$  [103]. Models based on this approach [68,100–111] differ mainly in how they obtain the effective Born radii. Replacing the interatomic distance ( $r_{ij}$ ) by  $f_{ij}$  has the effect of decreasing the contribution of the term,  $(Q_i Q_j / r_{ij})(1 - 1/\epsilon_{\text{eff}})$  to the solvation energy as  $r_{ij}$  becomes small. The effective dielectric screening thus increases with the interatomic distance. It should be noted in this respect that the considerations that led to Eq. (21b) involved the assumption that  $\epsilon_{\text{eff}}$ , which is frequently taken as  $\epsilon_p$ , is the same for charge–charge interaction and Born's energy. This very problematic assumption should be kept in mind while assessing the meaning of the GB results.

Generalized Born models have given encouraging results in MD simulations of proteins [68,107,110] and for solvation energies of simple ions in solution, but have not yet been tested extensively for other problems in protein electrostatics. It is important to note that Eq. (22) is not a mathematical solution to

the problem of charges in a multicavity continuum, or of a system with multiple dielectric regions such as a protein surrounded by water [8]. Although an increase in dielectric screening with distance is in accord with experiment, there is no sound theoretical basis for Eq. (22) or (23). Nor does the model prescribe a unique value of  $\epsilon_{\text{eff}}$  to use with Eq. (22) in applications to proteins, although values of at least 20 probably will be needed in most cases.

The above discussion shows that the GB treatment is an approximation of Eq. (16) and thus does not go much beyond Coulomb's law [8]. Nevertheless, it is instructive to note that the GB approximation also can be obtained by assuming a local model in which the vacuum electric field,  $\mathbf{E}_0$ , and the displacement vector,  $\mathbf{D}$ , are identical [113]. This model can be considered as a "local Langevin Dipole model" [69] or as a version of the non-iterative LD model. The GB approximation emerges if one uses this model to approximate the energy of a collection of charges and makes some additional assumptions about the position dependence of the dielectric constant.

Eq. (19) is valid only for homogeneous media with a high dielectric constant. We cannot assume that it will apply as well to transfer of charges from water to a protein. A more consistent treatment requires replacing  $\Delta G_{\text{sol}}^{\infty}$  by the free energies of the individual ions in their protein sites, where the effective value of  $\epsilon$  is variable. Fortunately, however, it usually is reasonable to use a large  $\epsilon_{\text{eff}}$  for the second term in Eq. (19), even for protein interiors. Here again, the main issue is the reliability of Eq. (21) and not its legitimization by a seemingly rigorous GB formulation.

Unlike the GB model, Eq. (16) does not attempt to capture the term  $G_{\text{sol}}^{\infty}$  along with the charge–charge interaction term by a single sum. There are, however, many situations, in which  $G_{\text{sol}}^{\infty}$  is either constant, or can be removed by a suitable thermodynamic cycle, leaving the charge–charge interactions as the factor of interest. The effects of mutations on the  $\text{p}K_{\text{a}}$  of another residue or on the  $E_{\text{m}}$  of a bound cofactor exemplify such situations.

#### 4. The meaning of protein dielectric constants

It is often assumed that the dielectric constant of proteins ( $\epsilon_{\text{p}}$ ) is a universal quantity that can be used in a variety of models. In particular, it was assumed for many years that proteins could be represented by a low dielectric constant in the range of 2 to 4, and this assumption was supported by several microscopic simulations (see below). However, a microscopically-based conceptual and practical analysis by Warshel and Russell [12] indicated that the value of  $\epsilon_{\text{p}}$  is entirely dependent on the method and system used to define this quantity. This initially appeared to be a questionable conclusion, and it still might look strange to readers who are accustomed to the view that macroscopic models have a universal physical meaning. It may also be puzzling to workers who are experienced with microscopic statistical mechanics, where  $\epsilon$  (usually called  $\bar{\epsilon}$ ) can be evaluated in a unique way from the fluctuations of the total dipole moment of the system (see below). Even now it is not widely recognized that the best value of the parameter  $\epsilon_{\text{p}}$  to use in modeling electrostatic effects has

little to do with what is usually considered as the protein's dielectric constant. Systematic studies [13,19,114] have shown that  $\epsilon_{\text{p}}$  is basically a measure of all the electrostatic interactions that are not included explicitly in the model. This point can be appreciated by considering several limiting cases. If all the interactions are treated explicitly,  $\epsilon_{\text{p}}=1$ ; if all but induced dipoles are included explicitly,  $\epsilon_{\text{p}}\approx 2$ ; and if the solvent is not included explicitly (a very poor model),  $\epsilon_{\text{p}}>40$ . If the protein's permanent dipoles are included explicitly but the protein's induced dipoles and relaxation of the permanent dipoles around the charged groups (the protein reorganization) are treated implicitly, the value of  $\epsilon_{\text{p}}$  is not a well-defined quantity. The most appropriate value of  $\epsilon_{\text{p}}$  in this situation usually is between 4 and 6 for dipole–charge interactions and between 4 and 10 for charge–charge interactions [115,116]. In general, the effective dielectric constant in protein interiors is not a constant because it depends on the site considered as well as the model [114,117].

Several authors have argued that there is only one 'proper' dielectric constant, which is the statistical mechanical dielectric constant ( $\bar{\epsilon}$ ), obtained from the fluctuations of the average total dipole moment of a system [6,114,117–120]. However, this dielectric 'constant' is not constant, since it depends on the specific region in the protein [114,117]. It is also sometimes assumed that  $\epsilon_{\text{p}}$  is equal to  $\bar{\epsilon}$ , but this assumption is completely unjustified. For example, using an explicit model frequently produces  $\bar{\epsilon}>6$ , while, as discussed above, one has to use  $\epsilon_{\text{p}}=1$  when all interactions are treated explicitly (see Ref. [121] for detailed discussion). The relatively large value of  $\bar{\epsilon}$  is frequently assumed to reflect fluctuations of ionized groups on the surface of the protein [69,117,120,122]. However, recent experimental studies [99,123,124] have supported the theoretical finding [114] that active sites in proteins generally have large values of  $\bar{\epsilon}$ , even when these sites are far from the surface.

Although the misconceptions about  $\bar{\epsilon}$  have been reviewed elsewhere [19], it is nevertheless useful to summarize what has been learned about  $\bar{\epsilon}$  for proteins. The value of  $\bar{\epsilon}$  apparently can be significantly larger than the value of about 4 deduced from measurements of the dielectric properties of dry proteins and peptide powders [125,126], or from simulations of the entire protein rather than a specific region [114]. The early theoretical finding of  $\bar{\epsilon}\approx 4$  in a gas-phase study [126], ignored the effect of the reaction field of the solvent. This type of treatment drastically underestimates the value of  $\bar{\epsilon}$  (see discussion and demonstration in [114]). Simulations by King et al. [114] that included the solvent's reaction field gave  $\bar{\epsilon}\approx 10$  in and near the active site of trypsin. Similar values were obtained even in the absence of fluctuations of the ionized residues on the protein's surface, showing that polar groups and water molecules in interior regions contribute significantly to  $\bar{\epsilon}$ . It was suggested recently that the calculations by King et al. [114] may not have converged [9], but the SCAAS model that was used actually converges much more rapidly than the periodic models (and the corresponding very large simulation systems) used in the presumably "converging" studies mentioned in ref. [9], and the convergence of  $\bar{\epsilon}$  was examined by longer runs and by using alternative formulations. To our knowledge, however, there have been no attempts to repeat the calculations of  $\bar{\epsilon}$  by King

et al. [114] for trypsin or any other enzyme. Thus, it seems that the main obstacle to reaching a consensus about  $\bar{\epsilon}$  is the undue impact of studies (e.g., [117,127]) that considered the entire protein instead of specific regions, and the attempt to deduce the effect of ionized surface groups by evaluating  $\bar{\epsilon}$  in specific protein regions when the surface groups are neutral.

Despite the intrinsic interest in the nature of  $\bar{\epsilon}$ , the above analysis indicates that this quantity is not highly relevant to the energetics of charges in proteins and does provide a unique way of determining  $\epsilon_p$  for a semimacroscopic model. Another good way to appreciate this point is to consider a charge in a water sphere surrounded by water. In such a model,  $\bar{\epsilon} \approx 80$ , whereas a microscopic model of the same system with implicit induced dipoles will require  $\epsilon_p \approx 2$ .

One could argue reasonably that the entire concept of a dielectric constant is invalid in the heterogeneous interior of a protein [11]. However, since fully microscopic models still do not give sufficiently precise results, it is useful to be able to estimate electrostatic energies using implicit models and, in particular, semimacroscopic models. Thus, it is justified to look for optimal  $\epsilon_p$  values after realizing what this parameter really means. In principle, the semimacroscopic PDL/S-LRA model should use  $\epsilon_p \approx 2$  because all effects except those of the protein's induced dipoles are considered explicitly. However, the configurational sampling by the LRA approach obviously is not perfect. Although the protein reorganization energy probably is captured to a reasonable extent [121], the change in water penetration on ionization of charged residues probably is not reproduced accurately. This problem is particularly serious for ionizable groups in nonpolar sites in the interior of a protein. In such cases the ionization processes can cause significant changes in water penetration, as demonstrated in the instructive experiments of Garcia-Moreno et al. [128]. Molecular dynamics simulations are unlikely to reproduce these changes in nanosecond simulation times, without special tricks of the type described in Ref. [129] and Section 7.

That the effective dielectric constant for charge–charge interactions in proteins is larger than usually assumed has been pointed out by several workers [10,94,130]. However, this important observation has not always been analyzed with a clear microscopic perspective. Based on classical studies of water, Mehler and coworkers correctly argued [94,96] that in polar solvents the effective screening factor,  $\epsilon_{\text{eff}}^j$  of Eq. (16) is a sigmoidal function that increases to a large value at relatively short distances [131–133]. Jonsson and coworkers [130] assumed that electrostatic interactions in proteins can be described by using a large  $\epsilon_p$  for charge–charge interactions. Although we completely agree that  $\epsilon_p$  and  $\epsilon_{\text{eff}}$  frequently are large [10,12], we believe that the reasons for this are more subtle than is generally realized. It is important to note that the behavior of  $\epsilon_{\text{eff}}(r)$  in water is not necessarily relevant to the corresponding behavior in proteins, where many of the permanent dipoles have more restricted mobility. The surprising observation that charge–charge interactions are strongly screened in proteins was rationalized by Warshel and Russell [12], who pointed out that the screening must reflect the compensation of charge–charge interactions and solvation

energy. Qualitatively, as two charges come closer together, the increase in their direct Coulombic interaction is offset by a decrease in the sum of their individual solvation energies. For an illustration of this effect, see Fig. 4 of Sham et al. [115]. The compensation is nearly perfect in water and other polar solvents, where the electrostatic free energy of an ion pair is virtually independent of the distance between the ions, and it holds surprisingly well down to 5 or 10 Å even in proteins. It seems to us that understanding this crucial compensation effect is essential for an understanding of  $\epsilon_p$  in proteins.

Baptista and coworkers [134], addressed the idea that PB models should use two different dielectric constants: one for self energies (called  $\epsilon_{\text{ind}}$  in their paper) and the other for charge–charge interactions (called  $\epsilon_{\text{pair}}$ ). They tested this proposition with values of 4 and 20 for  $\epsilon_{\text{ind}}$  and  $\epsilon_{\text{pair}}$ , respectively, using a PB model that did not include relaxations of the protein. The authors noted that our early work [54] had suggested that the effective dielectric constants for charge–dipole and charge–charge interactions are generally different. However, we did not mean to imply that the problems in using PB models without relaxations of the proteins can be fixed by using a lower dielectric constant for computing self energies. In fact, we pointed out that the problems of PB models with unrelaxed proteins and low dielectric constants cannot be fixed, and that one must use the PDL/S-LRA or related treatment in order to have any hope of finding a relatively uniform dielectric scaling. In other studies, we found that unrelaxed PB treatments require a value of about 10 for  $\epsilon_{\text{ind}}$  [115].

As we would expect, and as shown in our works, the use of 4 and 20 for  $\epsilon_{\text{ind}}$  and  $\epsilon_{\text{pair}}$ , respectively, by Baptista and coworkers [134] gave very poor results. Better results were obtained by using a protein dielectric constant of about 20 for all interactions. Unfortunately, the authors took these results to mean that our proposal is incorrect. It was then argued that the problem with the proposal is the assumption that our  $\epsilon_{\text{eff}}$  is equal to  $\epsilon_{\text{pair}}$ . In protein interiors,  $\epsilon_{\text{pair}}$  is, in fact, quite close to the  $\epsilon_{\text{eff}}$ . It is smaller near the surface, since  $\epsilon_{\text{eff}}$  implicitly includes the effect of the solvent.

Using  $\epsilon_{\text{ind}}=20$  for treating self-energies may not be a good idea even with PB treatments of charges in unrelaxed protein interiors. One of the best examples of the problem is provided by calculations of the redox potential ( $E_m$ ) of cytochrome *c*. One cannot obtain the large shift of the  $E_m$  relative to the  $E_m$  of the reference model compound in water, unless  $\epsilon_{\text{ind}}$  is smaller than 6 [121]. Of course, we cannot provide general universal rules for the inconsistent unrelaxed PB models, but  $\epsilon_{\text{ind}}$  should definitely be smaller than  $\epsilon_{\text{pair}}$  in consistent semimacroscopic models.

Contrary to what one might assume, the effective macroscopic dielectric constant for a given region in a protein cannot be used to provide a general description of the energetics of charges in this region [120]. The conceptual problem with this assumption is illustrated in Fig. 3. The figure represents an internal site in which a charged group interacts with a dipole that is fixed in position and a second dipole that is free to rotate. Since this is an internal site, the leading term in semimacroscopic treatments will be the

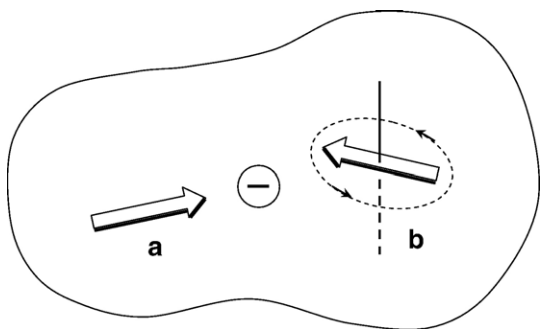


Fig. 3. A single macroscopic dielectric constant cannot be used to reproduce the energetics of charges in proteins in a unique way. The figure shows a hypothetical site with a negative charge, a fixed dipole (a) and a freely rotating dipole (b). Using the same  $\epsilon_p$ , obtained by microscopic calculations of the reorganization energy, for both dipoles will underestimate the interaction of the charge with dipole a and overestimate the interactions with dipole b.

$\Delta U_{\text{QM}}/\epsilon_p$  term of Eq. (13). One of the best ways to estimate  $\epsilon_p$  is to calculate the reorganization energy associated with introducing the charged group [9,121]. However, using this  $\epsilon_p$  in Eq. (13) will underestimate the interaction of the charge with the fixed dipole, while overestimating the interaction with the rotating dipole. The same problem will occur if we use the  $\bar{\epsilon}$  evaluated from the dipolar fluctuations in the region that includes both the dipole and the charge. Furthermore, if the site involved an ion pair instead of a single ionized group we would need a different  $\epsilon_p$  to reproduce the electrostatic free energy of the ion pair.

### 5. Examining the reliability of electrostatic calculations

As one can see from the previous sections, accurate evaluations of electrostatic energies in proteins are far from trivial. However, the problems associated with some models have been obscured by the use of inappropriate validation procedures. An example is the use of  $pK_a$  calculations to validate electrostatic models. Although  $pK_a$  value calculations, in principle, provide an effective way to examine the performance of electrostatic models [12,44,50,55,96,122,128,135], most studies have focused mainly on the  $pK_a$  values of surface groups, which generally are the most accessible to experiment. Unfortunately, most of these  $pK_a$  values are not very different from the values for the same groups in water and can be reproduced by many models, including some that are fundamentally incorrect [8]. The use of unweighted  $pK_a$  values for a large number of proteins as a benchmark thus is likely to lead to unjustified conclusions. It has been pointed out [8,128] that ionizable groups in protein interiors should provide much more discriminating benchmarks, because these groups reside in very heterogeneous environments where the interplay between polar and nonpolar components is crucial. For example, an ionizable group in a truly nonpolar environment will have an enormous  $pK_a$  shift that cannot be reproduced well by models that assume a high dielectric in the protein interior. Similarly, a model that describes the protein as a medium with a uniform low dielectric, without permanent dipoles, will not work well if the environment around the ionizable group is polar [12].

The problems with non-discriminating benchmarks were established by Schutz and Warshel [19] and are illustrated in Fig. 4. This figure considers the  $pK_a$ s of a set of acidic and basic residues and correlates the results obtained by the modified TK (MTK) model with  $\epsilon_p=40$  and  $\epsilon_{\text{eff}}=80$  (see [19]) with the observed  $pK_a$ s for the same residues. The upper plot gives the impression that the MTK is an excellent model. The same impression was given by influential studies of  $pK_a$  in proteins [122]. However, essentially the same agreement would be obtained with any model that uses a large  $\epsilon$ , since most surface Asp and Glu residues have  $pK_a \approx 4$  and most surface Lys residues have  $pK_a \approx 10$ . Thus, as emphasized in the lower graph in the figure, we have very little useful information, and the best correlation would have been obtained with the trivial null model in which  $\Delta pK_a=0$  for all surface groups.

As this example illustrates, it is essential to validate  $pK_a$  calculations by using discriminative benchmarks with  $|\Delta pK_a| > 2$  and to use the same philosophy for other electrostatic properties. The use of such discriminative benchmarks in  $pK_a$  calculations has proven to be extremely useful for demonstrating the range of validity and the best values of  $\epsilon_p$  for different models [19].

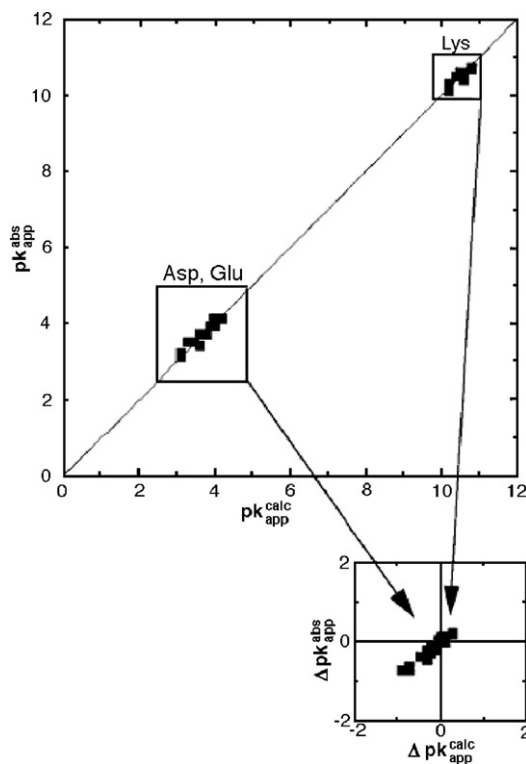


Fig. 4. The correlation between calculated and the observed  $pK_a$  values gives a nondiscriminative benchmark if all the experimental values are for surface groups. The figure considers surface Asp, Glu and Lys residues for which the measured  $pK_a$  value in the protein ( $pK_{\text{app}}^{\text{obs}}$ ) is similar to that for the same functional group in solution. The calculated  $pK_a$  values ( $pK_{\text{app}}^{\text{calc}}$ ) are evaluated by the MTK(S) model with  $\epsilon_p=40$  and  $\epsilon_{\text{water}}=80$ . A plot of  $pK_{\text{app}}^{\text{obs}}$  vs.  $pK_{\text{app}}^{\text{calc}}$  (upper graph) shows seemingly impressive results for this benchmark, but when the results are displayed as the difference between the  $pK_a$  values in the protein and in solution ( $\Delta pK_{\text{app}}^{\text{obs}}$  vs.  $\Delta pK_{\text{app}}^{\text{calc}}$ , lower graph) it becomes clear that we simply have a poor benchmark. Because all the  $\Delta pK_a$  values are small, any model that produces a small  $pK_a$  shift looks like an excellent model. Adapted from [19].

A recent study of the PMF for ion penetration through ion channels [57] provides another example of validation of electrostatic models. The issue here is the validity of seemingly rigorous statistical mechanical expressions such as Eq. (11), and the problem again is that such approaches have been examined only by using insufficiently discriminating benchmarks such as the torsional potential of the alanine dipeptide rather than systems with the necessary electrostatic heterogeneity. Furthermore, calculations on an actual ion channel cannot be considered a proper benchmark because it is not clear a priori what is necessary in order to obtain converging results in such a system. This problem was addressed by Kato and Warshel [57], who used part of a gramicidin channel with a variable number of water molecules to establish a system that provided converging simulations (Fig. 2). Comparing the PMF for moving an ion through or around this channel, which should be identical, provides a way of assessing the hysteresis in the calculations (see Fig. 2).

## 6. Calibrating calculations by studies of solvation energies of small molecules

Modeling a biological process can be helped enormously by calibrating the calculated free energy change relative to the observed or estimated free energy of a corresponding process in aqueous solution [12,136]. This is especially important for enzymatic reactions, where the catalytic effect is defined relative to the solution reaction. It also applies to calculations of ligand-binding processes, where one has to compare the solvation energy of the ligand in its protein site to the corresponding solvation energy in solution. Early attempts to estimate solvation energies [137,138] were based on Born's expression for the energy of a charge in a spherical cavity with a basically arbitrary radius (Eq. (20)) or Onsager's similar expression for a dipole. The first attempts to move toward quantitative evaluation of solvation energies branched in two directions. One approach was to examine the interaction between the solute and a single solvent molecule quantum mechanically [139,140]. The other approach, which ultimately turned out to be the more successful, was to parameterize the solute–solvent van der Waals interactions in a complete solute–solvent system empirically, and evaluate the interaction between the solute and many (rather than one) solvent molecules [37]. Although the empirical approach was regarded initially as having “too many parameters,” it was realized eventually that having an atom–solvent parameter for each type of solute atom is the key requirement in any quantitative semiempirical solvation model. Recent continuum solvation models [141–143] have essentially the same number of parameters as current all-atom models [40,51,52,144]. For a solute with a given set of charges, the crucial step in either type of model is parameterization of the solute–solvent repulsion term or the corresponding atomic radius (see [25]). Leaving the selection of reasonable parameter values aside, the next requirement is to obtain converging results with the particular modeling method that is chosen.

The general progress in modeling solvation energies of small molecules and ions is quite encouraging, as is apparent from the results reported by many research groups using a variety of

simulation approaches. FEP calculations have focused on the proper treatment of ionized groups and the importance of proper boundary conditions [26,27,33,40,145]. Recently, the validity of the LRA treatment [53] in solvation calculations was explored [146] and the LRA formalism was used in a quantum mechanical treatment [147]. LD calculations were found to give accurate results when incorporated into quantum mechanical models [148,149] and similar success was reported in continuum [141,150] and GB studies [104]. All of these models apparently give similar accuracy once properly parameterized. The deviation from experiments after reasonable parameter fitting in some cases could reflect the neglect of charge transfer to the solvent.

These successful calculations on small molecules in solution could be viewed as almost trivial in one sense, considering that the environment is uniform and the solvation can be related to the effective atomic radius in a simple way. Unfortunately, the ability to reproduce solvation energies in solution does not guarantee that the same treatment will give reliable results for solvation energies of ligands in proteins, or for the solvation energy of the entire macromolecule.

## 7. Evaluation of $pK_a$ s of ionizable residues in proteins

Ionizable residues in proteins play major roles in almost all biological processes, including enzymatic reactions, proton pumps and protein stability. Understanding these roles can require evaluating both the interactions of the ionized groups and the energetics of the ionization process itself. Thus an ability to calculate  $pK_a$ s of ionizable groups in proteins can be crucial for structure–function correlations as well as for validating different treatments of electrostatic energies [12].

Calculations of  $pK_a$ s by all-atom FEP approaches have been described for only a small number of proteins [50,56]. Recent work includes studies of the  $pK_a$  of metal-bound water molecules [151] and proton transfer in proteins [152] as well as functionally important groups [153–156]. Several all-atom LRA calculations also have been described [54,55]. PDL/D/S-LRA calculations have given encouraging results with  $\epsilon_p=4$  [19,54]. Although the LRA treatment considers the protein reorganization formally, the limit of  $\epsilon_p=2$  expected for a “perfect” model with implicit induced dipoles has not been reached, probably because some of the reorganization and/or water penetration is not captured in the computer time used in the simulations. Only a few studies (e.g. [36]) include estimates of the error range in the calculations. It appears that the error range of the all-atom models is still somewhat disappointing and that in some cases the results of microscopic calculations are simply disastrous, which perhaps explains we have so few reported studies. However, inclusion of proper long-range treatments and induced dipoles does lead to some improvements [54,56].

Semimacroscopic-continuum models, such as the current version of the PB models, which now include the protein permanent dipoles and the self-energy term, frequently give reasonable results. Yet most PB models [122,157,158] do not treat the protein reorganization explicitly, and the so-called multi-conformation continuum electrostatic (MCCE) variant [87] considers only the reorganization of polar side chains rather

than including a proper average over all the protein coordinates. As discussed in Sections 3.4 and 4, a problem with most current PB models is the use of the same  $\epsilon_p$  for interactions with of the ionizable group with protein dipoles and for charge–charge interactions [19,54]. This requirement leads to inconsistencies that may not be apparent in the absence of discriminating benchmarks for both self-energies and charge–charge interactions. Trends in  $pK_a$  changes, however, frequently can be captured by models that focus mainly on charge–charge interactions rather than on the self-energy term, or that estimate the self-energy term by empirical considerations [96].

There appears to be a common perception that the main problem in continuum calculations of  $pK_a$  is the need for averaging over the protein configurations [159–161]. The obvious need for proper configurational averaging in free energy calculations should not be confused with dynamics effects, as has been done in several cases (e.g., [162]). Perhaps more importantly, many attempts at configurational averaging have considered only the charged state of the ionizable residue. This amounts to using only one charge state in the LRA treatment (Eq. (9)) and leads to incorrect estimates of the charging free energy. It is important to recognize that a proper LRA averaging over both charge states is essential for formally correct  $pK_a$  calculations.

A more complete consensus on the validity of different models for  $pK_a$  calculations may not be obtained until the microscopic models start to give stable quantitative results. Comparing microscopic and semimacroscopic models as was done by Sham et al. [54] will be helpful in this regard. Before moving forward, however, it is important to try to resolve the major challenges introduced by cases where microscopic calculations do not reproduce the observed electrostatic effects. A good example is the  $pK_a$  of Glu 66 in the hydrophobic site of staphylococcal nuclease, which has been a major challenge for microscopic calculations [163,164]. Our attempt to obtain the  $pK_a$  of Glu 66 by the standard FEP approach also gave a major deviation from the observed  $pK_a$  (a predicted shift of 23 units instead of 5), despite the use of relatively long (5 ns) simulations. This suggests that ionization of Glu 66 is accompanied by local unfolding of the protein and/or a substantial penetration of water. The problem is to capture this configurational change within practical simulation times [129]. To address this challenge we have developed a new “overcharging” cycle in which the conformational change is induced by changing the charge from 0 to a value ( $Q_i$ ) below  $-1$  and then returning it to  $-1$ .  $Q_i$  is varied to minimize the overall free energy change in the two steps. The free energy of changing the charge from 0 to  $-1$  is evaluated as:

$$\Delta G(Q = 0.0 \rightarrow Q = -1.0) = \min[\Delta G(\mathbf{r}_0, Q = 0 \rightarrow \mathbf{r}_i, Q = Q_i) + \Delta G(\mathbf{r}_i, Q = Q_i \rightarrow \mathbf{r}_i, Q = -1.0)] \quad (24)$$

where  $\mathbf{r}_i$  is the protein structure generated by charging up to  $Q_i$ . The first term on the right hand side of Eq. (24) is obtained from the PMF for moving from  $\mathbf{r}=\mathbf{r}_0$  and  $Q=0.0$  to  $\mathbf{r}=\mathbf{r}_i$  and  $Q=Q_i$ ; the second term, from the PMF for moving from  $Q=Q_i$  to  $Q=-1.0$  with  $\mathbf{r}=\mathbf{r}_i$ . Performing such a charging and uncharging cycle with  $Q_i=-2.0$  led to a remarkable hysteresis that can be

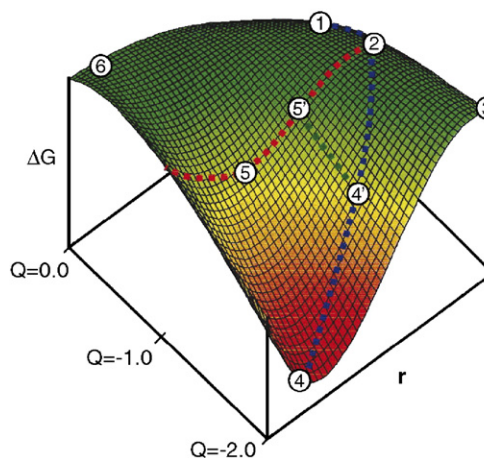


Fig. 5. A schematic illustration of an overcharging procedure. The figure shows the free energy surface as a function of the charge ( $Q$ ) of an ionizable residue and an effective protein coordinate ( $r$ ). The mapping procedure evaluates  $\Delta G_{1 \rightarrow 5}$  by calculating  $\Delta G_{1 \rightarrow 5'} = \Delta G_{1 \rightarrow 4'} + \Delta G_{4' \rightarrow 5'}$  and then finding the lowest  $\Delta G_{1 \rightarrow 5'}$ . Adapted from [129].

seen by inspection of Fig. 5. Examining the structures from different charging cycles showed that charging to  $Q_i=-2.0$  leads to a drastic unfolding and a complete exposure of the ionized Glu residue to the solvent. A gradual cycle that reached  $Q_i=-1.7$  led to a small local change and water penetration. Since the overcharging procedure generates different sets of protein structures corresponding to different degrees of charge-induced reorganization, we can use these structures to explore the relationship between the protein landscape and the energetics of the ionization. The full procedure is described elsewhere [129]. Although our findings require further validation, they clearly indicate that water penetration may play a major role in the observed  $pK_a$  of Glu 66. The use of such an artificial charging process to simulate a physically meaningful structural change may be an exciting new strategy that could, for example, provide the breakthrough needed for obtaining reliable results on hydrogen exchange in proteins (for a review of the latter field, see [165]).

## 8. Redox potentials and electron-transfer processes in proteins

Electron transfer reactions are involved in key energy transduction processes in living systems including, most notably, oxidative phosphorylation and photosynthesis. These processes involve changes in the charges of the electron donor and acceptor, and thus are controlled partly by the electrostatic energies of the charged groups. Here the challenge is to evaluate the redox energies and reorganization energies using the protein structure. Probably the first to address this problem was Kassner [166,167], who represented the protein as a nonpolar sphere. The idea that such a model can be used for analyzing redox properties of proteins held up until the mid 1980s (see the discussion in [74,168–174]), when Warshel and coworkers showed by using the PDL model [175,176] that evaluations of redox potentials must take into account the protein’s permanent dipoles and internal water molecules. The importance of the permanent dipoles was established clearly in subsequent studies

of iron–sulfur proteins [177,178]. Another interesting factor is the effect of ionized residues on redox potentials, which often can be described well using Coulomb’s law with a large effective dielectric constant (Eq. (16)) [10,45,99,128].

Microscopic estimates of protein reorganization energies have been described [45,121,179,180] and have been used in studies of the rate constants of biological electron transport. This also includes studies of nuclear quantum mechanical effects associated with fluctuations of the protein’s polar groups (for review see [181]). PB studies of redox proteins also have progressed significantly [82,168,171,182,183], although some confusion still appears to persist on the importance of the protein permanent dipoles (see discussion in [74,168]).

To illustrate some of the complexities associated with calculations of electrostatic free energies in redox proteins, it is instructive to consider computational studies of the initial electron-transfer step in photosynthetic bacterial reaction centers (RC’s). The elucidation of the crystal structure of this system presented major challenges to both computational and experimental approaches. An immediate question was whether the initial event involved stepwise electron transfer from an excited bacteriochlorophyll dimer ( $P^*$ ) to a neighboring bacteriochlorophyll ( $B_L$ ), followed by electron transfer from  $B_L^-$  to a bacteriopheophytin ( $H_L$ ), or a superexchange process in which  $P^*$  transferred an electron directly to  $H_L$  with the assistance of electronic coupling to  $P^+B_L^-$  as a virtual intermediate. In the two-step mechanism,  $P^+B_L^-$  would have to lie close to or below  $P^*B_L$  in energy, while superexchange would allow  $P^+B_L^-$  to be at a higher energy. Microscopic FEP/US and PDL calculations that included proper treatments of boundary conditions and long-range interactions gave similar energies for  $P^*B_L$  and  $P^+B_L^-$ ,

supporting the two-step mechanism [45,184,185]. However, studies by other workers put  $P^+B^-$  much higher in energy and appeared to favor the superexchange mechanism [186–188]. The two-step mechanism ultimately was confirmed experimentally, and the conflicting results from some of the calculations were shown to stem from an incomplete treatment of dielectric effects (see discussion in Refs. [45,189]).

Our more recent calculations have lent further support to the two-step mechanism [14,181]. Fig. 6A shows the results of FEP/US calculations for electron transfer from  $P^*$  to  $B$  in *Rhodobacter sphaeroides* RCs. The curves plotted with thin lines were obtained from separate MD simulations on the potential energy surfaces of the reactant ( $P^*B_L$ ) and product ( $P^+B_L^-$ ) state, respectively. These free-energy curves are most reliable in the regions of their potential minima, where the system spends most of its time during the trajectory. Sampling of the region between the two minima can be improved by combining the results from the two trajectories. Taking the minimum free energy of  $P^*B$  as zero, the averaged free energy function (Eq. (8)) for this state becomes

$$\Delta g_{P^*}(x') = -k_B T \ln \left\{ \frac{1}{2} \left[ \frac{\langle \delta(x - x') \rangle_{P^*}}{\langle \delta(x - \langle x \rangle_{P^*}) \rangle_{P^*}} + \exp(\beta x' - \beta \Delta G_{P^* \rightarrow P^+B^-}^0) \times \frac{\langle \delta(x - x') \rangle_{P^+B^-}}{\langle \delta(x - \langle x \rangle_{P^+B^-}) \rangle_{P^+B^-}} \right] \right\} \quad (25)$$

Here the reaction coordinate ( $x$ ) is the energy difference between the diabatic product and reactant states, which

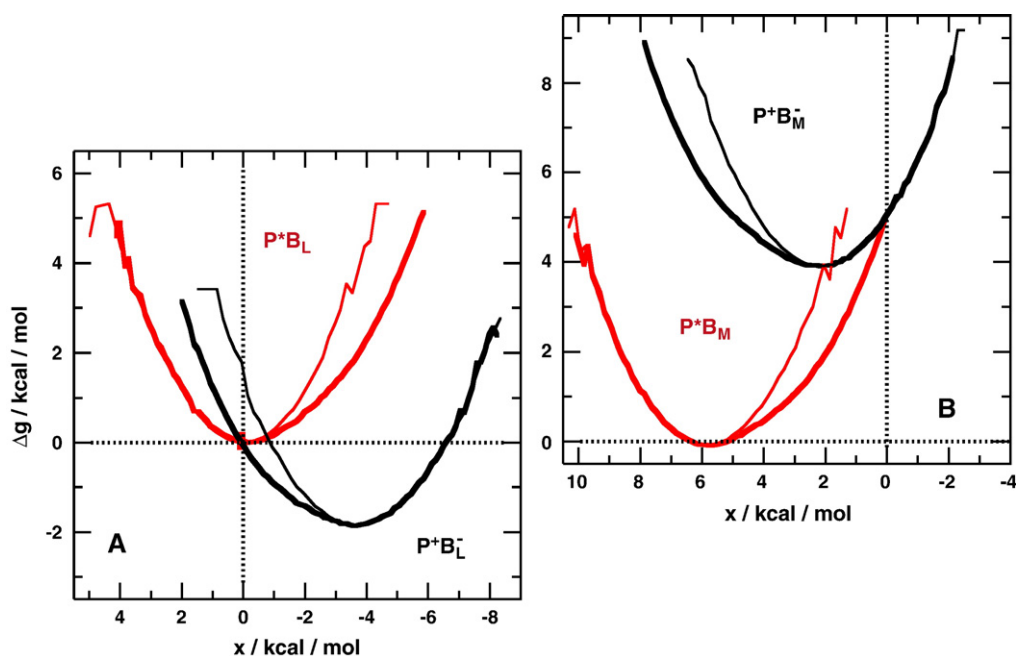


Fig. 6. (A) Calculated free-energy functions for the diabatic reactant ( $\Delta g_{P^*}$ , red) and product ( $\Delta g_{P+B}$ , black) states in the reaction  $P^*B_L \rightarrow P^+B_L^-$  in *Rb. sphaeroides* reaction centers. The abscissa is the reaction coordinate, which is defined as the electrostatic energy difference between the two states. The free-energy functions plotted with thin lines were obtained by Eq. (27) from separate MD trajectories on the two potential surfaces; those plotted with thick lines were obtained by combining the results from these trajectories (Eq. (25)). (B) Same as (A) but for the reaction  $P^*B_M \rightarrow P^+B_M^-$ . Adapted from [14].

fluctuates with time during the MD trajectories, and  $\Delta G_{P^* \rightarrow P^+B^-}$  is the overall free-energy change given by the FEP calculations ( $-1.9$  kcal/mol). The free-energy function for  $P^+B^-$  is obtained similarly. The calculated free energies of the two states are plotted with thick lines in Fig. 6. If  $|\Delta G_{P^* \rightarrow P^+B^-}|$  were much larger, trajectories on additional mapping potentials would be required in order to sample the configurational space between the two minima adequately.

One way to check whether the conformational space is sampled sufficiently well in a given region of the reaction coordinate is to see whether the free-energy functions for the reactant and product states satisfy the expression (see Ref. [52])

$$\Delta g_\beta(x) = \Delta g_\alpha(x) + x, \quad (26)$$

which follows from the relationship [52,190],

$$\Delta g_\beta(x') = -k_B T \ln[\langle \delta(x - x') \exp(-x/k_B T) \rangle_\alpha / \langle \delta(x - \langle x \rangle_\alpha) \rangle_\alpha] \quad (27)$$

The averaged free-energy curves plotted with thick lines in Fig. 6A conform to Eq. (26) in the region between the two minima, while the individual curves with thin lines do not.

Eqs. (26) and (27) indicate that the entire free-energy curve for the product state can be obtained from a sufficiently long MD trajectory in the reactant state and vice versa. However, these expressions assume that the trajectory samples the entire configurational space adequately, which is unlikely to be the case for a complex system [180,191]. A single trajectory on the reactant surface generally will not visit all the configurations that contribute significantly to the product surface, even if the overall free-energy change in the reaction is relatively small. Attempting to generate both free-energy surfaces from a single trajectory, therefore, is not recommended in most cases.

Fig. 6B shows the results of similar FEP calculations for electron transfer from  $P^*$  to the neighboring bacteriochlorophyll on the “inactive” branch of electron carriers ( $B_M$ ). The product state ( $P^+B_M^-$ ) is found to lie about 4 kcal/mol above  $P^*$ . This result agrees with the PDL calculations on RCs from the related species *Blastochloris viridis* [185], and is in good accord with the experimental finding that electron transfer occurs predominantly to  $B_L$  and  $H_L$  in preference to  $B_M$  and  $H_M$ . However, Ceccarelli and Marchi [192] have described MD simulations that put  $P^+B_M^-$  about 7 kcal/mol below  $P^*$ . The discrepancy with our calculations and experimental findings seem likely to stem from their use of periodic boundary conditions, and an Ewald-sum treatment of electrostatic interactions. They also propagated trajectories only on the reactant state and did not employ FEP, but that is less likely to account for the discrepancy. Clearly, fundamental flaws in a model cannot be remedied simply by increasing the number of atoms or the length of the MD trajectory, without critical validation studies. As stated in the previous section, the use of the spherical SAACS and LRF treatments is more reliable than the use of very large systems with periodic boundary conditions.

Despite the successes of consistent microscopic studies of RCs, it is useful to examine the validity of the results by comparison with an appropriate macroscopic model. We start by

noting that the free energy change for a reaction such as  $PB \rightarrow P^+B^-$  can be described macroscopically as

$$\Delta G_{\text{elec}} = \Delta E_{\text{gas}} + \Delta G_{\text{sol}}^\infty + \Delta U_{Q\mu}/\epsilon, \quad (28a)$$

where  $\Delta E_{\text{gas}}$  is the change in the vacuum molecular orbital energies of the electron donor and acceptor,  $\Delta G_{\text{sol}}^\infty$  is the change in solvation free energies of the electron carriers at infinite separation in a homogeneous medium with dielectric constant  $\epsilon$ , and  $\Delta U_{Q\mu}$  is the change in unscreened electrostatic interactions, including the direct interactions between the donor and acceptor ( $\Delta U_{QQ}$ ).  $\Delta E_{\text{gas}}$  can be estimated either by quantum calculations or by combining measured  $E_m$  values with calculated solvation energies [14,184,185]

$$\Delta E_{\text{gas}} = -F\Delta E_m - \Delta G_{\text{sol}}^{\text{ref}} \quad (28b)$$

We can use the Born equation (Eq. (20)) to relate the term,  $\Delta G_{\text{sol}}^\infty$ , to the corresponding free energy change in water or another reference solvent with a high dielectric constant,  $\Delta G_{\text{sol}}^\infty$ :

$$\Delta G_{\text{sol}}^\infty = \Delta G_{\text{sol}}^{w,\infty} + (1 - 1/\epsilon)/(1 - 1/\epsilon_w) \approx \Delta G_{\text{sol}}^{w,\infty} (1 - 1/\epsilon). \quad (29)$$

This approach is especially convenient if the same reference solution is used for calculating  $\Delta E_{\text{gas}}$  because it leads to cancellation of some terms in the final results. Combining Eqs. (28a) and (29) with Eq. (28b) and equating  $\Delta G_{\text{sol}}^{\text{ref}}$  with  $\Delta G_{\text{sol}}^{w,\infty}$ , the free energy change for the electron-transfer reaction becomes,

$$\Delta G_{\text{elec}} \approx -F\Delta E_m + (\Delta U_{Q\mu} - \Delta G_{\text{sol}}^{\text{ref}})/\epsilon. \quad (30)$$

Calculations using Eq. (30) have been described for the initial ion-pair states in *Bl. viridis* RCs [193]. Fig. 7 shows the calculated free energies of  $P^+B_L^-$  and  $P^+H_L^-$  relative to the ground state as functions of  $\epsilon$ . The horizontal dashed line indicates the energy of the excited state ( $P^*$ ). Experimentally,  $P^+H_L^-$  is found to lie about 6 kcal/mol below  $P^*$ , or about 23 kcal/mol above the ground state. The macroscopic model yields this result when  $\epsilon \approx 2.9$ . The microscopic PDL calculations mentioned above also reproduce the measured energy of  $P^+H_L^-$  without using an adjustable dielectric constant, but of course with much more effort. More significantly, Fig. 7 shows that any value of  $\epsilon$  that gives approximately the right free energy for  $P^+H_L^-$  puts  $P^+B_L^-$  between this state and  $P^*$ . This is a useful result in spite of the limitations of the macroscopic model, because it provides a back-of-the-envelope check on the PDL calculations, which also put  $P^+B_L^-$  between  $P^*$  and  $P^+H_L^-$ .

Perhaps the main point that emerges from simple models of this type is that the self energies of charged groups cannot be dismissed as small corrections to the electrostatic free energy. They sometimes dominate the problem. In the calculations of the free energy of  $P^+H_L^-$  shown in Fig. 7,  $\Delta G_{\text{sol}}^{w,\infty}$  ( $\Delta G_{\text{sol}}^{\text{ref}}$ ) is of the order of  $-77$  kcal/mol, which is similar to  $\Delta E_{\text{gas}}$ , about three times greater than  $F\Delta E_m$  [193]. Even for the charge-shift reaction  $P^+B_L^-H_L \rightarrow P^+B_L^-H_L$ , where there is no net change in electrical charge,  $\Delta G_{\text{sol}}^{w,\infty}$  is about  $-12$  kcal/mol, compared to 4 kcal/mol for  $\Delta E_{\text{gas}}$ ,  $-8$  kcal/mol for  $F\Delta E_m$  and  $-6$  kcal/mol

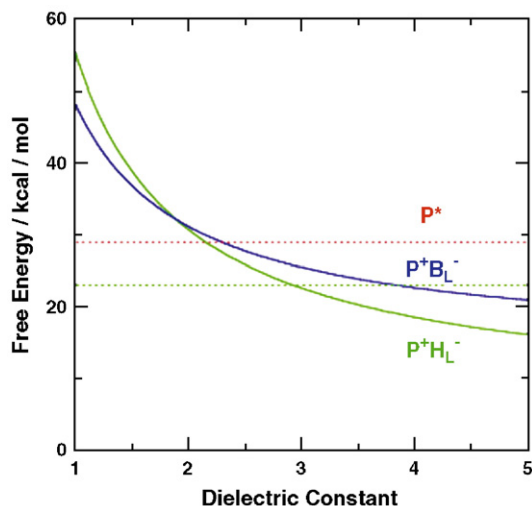


Fig. 7. Free energies of  $P^+B_L^-$  (blue curve) and  $P^+H_L^-$  (green curve) in *Bl. viridis* RCs as functions of the dielectric constant in a macroscopic model [193]. All energies in this figure are expressed relative to the ground state. The horizontal dashed red and green lines are, respectively, the energy of the first excited singlet state of P ( $P^*$ ) and an experimental value of the free energy of  $P^+H_L^-$ . The gas-phase energy for the reaction  $PH_L \rightarrow P^+H_L^-$  was obtained from the measured redox potentials of  $P/P^+$  and  $H_L^-/H_L$  and PDL calculations of the change in solvation energy for each of the half-cell reactions *in situ*; that for  $B_L + H_L^- \rightarrow B_L^- + H_L^-$  was obtained from the redox potentials of bacteriochlorophyll-*b* and bacteriopheophytin-*b* and the calculated solvation energies for the molecules in solution. The electrostatic free energy changes for  $PB_LH_L \rightarrow P^+B_LH_L^-$  and  $P^+B_LH_L^- \rightarrow P^+B_L^-H_L^-$  were calculated using Eq. (30) and were summed to obtain that for  $PB_LH_L \rightarrow P^+B_L^-H_L^-$ . See [193] for details.

for  $\Delta U_{Q\mu}$  [193]. Calculations that neglect the self-energies clearly should not be given much credence. The occasional ability of such calculations to reproduce an experimental result can be misleading in this respect, and, in most cases, probably can be traced to a cancellation of errors or to the choice of an indiscriminating benchmark; (see [45] for a discussion of how calculations by Marchi et al. [186], which omitted the solvent in and around the protein, gave what is almost certainly much too high an energy for  $P^+B_L^-$ , while fortuitously giving approximately the correct energy for  $P^+H_L^-$ ).

Another key question with regard to bacterial RCs is how slight asymmetries in the protein favor electron transfer from  $P^*$  mainly to  $B_L$  and  $H_L$  while blocking electron transfer to  $B_M$  and  $H_M$ . One possibility is that the specificity results from differences in electronic overlap of  $P^*$  with and  $B_L$  and  $B_M$ . However, as shown in Fig. 6, our PDL/S and FEP calculations indicated that the specificity probably is explained by the energetics of the two reactions, because the protein stabilizes  $P^+B_L^-$  significantly more strongly than  $P^+B_M^-$ . The calculations also identified some of the residues that contributed to the asymmetry of the energies [185]. These predictions have held up well to tests by studies of site-directed mutations that stabilize  $P^+B_M^-$  or destabilize  $P^+B_L^-$  (see, e.g., [194]).

Convergence of microscopic calculations proved to be a major problem in a recent quantum mechanical evaluation of the redox potentials of blue copper proteins [195]. In this case, semimacroscopic models presently give more accurate results than microscopic models.

## 9. Electrostatic effects in ligand binding to proteins

Reliable evaluations of the free energy of ligand binding can potentially make important contributions to structure-based drug design [196]. Here we have an interplay of electrostatic, hydrophobic and steric effects, but accurate estimates of the electrostatic contributions are still crucial.

In principle, it is possible to evaluate binding free energies by performing microscopic FEP calculations of the type considered in Eqs. (7) and (8). The difference between the free energies of gradually removing the force field from the ligand in the protein active site and in water should give the free energy of binding. This approach, however, encounters major convergence problems and, at present, the reported results have been disappointing except in cases of very small ligands. An alternative approach is to study the effect of small “mutations” of the ligand, such as replacement of  $NH_2$  by  $OH$  [51]. However, if one is interested in the absolute binding free energies for medium-size ligands, it is essential to use simpler approaches. Perhaps the most useful of these is the LRA approach of Eq. (9), augmented by estimates of the non-electrostatic effects.

The LRA approach is particularly effective for calculating electrostatic contributions to ligand binding energies [53,197]. In this approximation one can express the binding energy as

$$\Delta G_{\text{bind}} = \frac{1}{2} \left[ \langle U_{\text{elec},\ell}^p \rangle_{\ell} + \langle U_{\text{elec},\ell'}^p \rangle_{\ell'} - \langle U_{\text{elec},\ell}^w \rangle_{\ell} - \langle U_{\text{elec},\ell'}^w \rangle_{\ell'} \right] + \Delta G_{\text{bind}}^{\text{nonelec}}. \quad (31)$$

Here  $U_{\text{elec},\ell}$  is the electrostatic contribution to the interaction of the ligand with its surroundings; superscripts  $p$  and  $w$  designate protein and water, respectively; and  $\ell$  and  $\ell'$  designate the ligand in its actual charge form and the “nonpolar” ligand created by setting all its atomic charges to zero. In this expression the terms  $\langle U_{\text{elec},\ell} - U_{\text{elec},\ell'} \rangle$ , which are required by Eq. (9), are replaced by  $\langle U_{\text{elec},\ell} \rangle$  since  $\langle U_{\text{elec},\ell'} \rangle = 0$ . Evaluation of the nonelectrostatic contribution  $\Delta G_{\text{bind}}^{\text{nonelec}}$  is still very challenging, since these contributions might not follow the LRA. A useful option is to evaluate the individual contributions to the binding free energy from hydrophobic effects, van der Waals interactions, and water penetration [53,197].

Another powerful option is the so-called linear interaction energy (LIE) approach [198,199]. This approach adopts the LRA approximation for the electrostatic contribution but neglects the  $\langle U_{\text{elec},\ell'} \rangle$  terms. The binding energy is then expressed as,

$$\Delta G_{\text{bind}} \approx \alpha \left[ \langle U_{\text{elec},\ell}^p \rangle_{\ell} - \langle U_{\text{elec},\ell}^w \rangle_{\ell} \right] + \beta' \left[ \langle U_{\text{vdw},\ell}^p \rangle_{\ell} - \langle U_{\text{vdw},\ell}^w \rangle_{\ell} \right] \quad (32)$$

where  $\alpha$  is a constant that is approximately 1/2 in many cases and  $\beta'$  is an empirical parameter that scales the van der Waals (vdW) component of the protein–ligand interaction. While the general origin of the electrostatic scaling,  $\alpha$ , is relatively clear (it should be around 0.5 [53] with possible small deviations [146]),

the origin of the parameter  $\beta'$  and its general validity are much more problematic. This parameter appears to be different for different proteins, but to give reasonable results when held fixed for the binding of different ligands to the same protein [199]. Ref. [197] provides details of the relationship between the LRA and LIE approaches and discusses the overall non-electrostatic contributions (e.g., van der Waals, water penetration, hydrophobic and entropy contributions) that are represented by  $\beta'$ . The latter factor basically covers that part of the cycle that corresponds to binding of the nonpolar form of the ligand (while transfer of the polar or charged ligand to its nonpolar form is covered by the electrostatic part of the cycle). However, while Ref. [197] proposed a general way to explain the nature of  $\beta'$  in different systems and discussed how to predict  $\beta'$  for different active sites (see, e.g., Eq. (35) in Ref. [197]), it left actual studies to subsequent works. Nevertheless, Ref. [197] gave, at the end of its concluding remarks, a detailed rationalization as to why the LIE scaling with  $\langle U_{\text{vdw}} \rangle$  might be reasonable.

Åqvist and coworkers have demonstrated that the nonpolar contribution to the solvation in solution is proportional to  $\langle \Delta U_{\text{vdw}} \rangle$  [198] and, more recently, that the nonpolar contribution to the binding energy is approximately proportional to the size of the ligand and that  $\langle \Delta U_{\text{vdw}} \rangle$  also scales linearly with the ligand size [200]. Determining the generality and the quantitative nature of this finding will require further studies including assessment of the size dependence of the water penetration effect considered in Ref. [197].

More implicit models can, of course, be used to estimate the binding energy. These include the PDL/D/S-LRA model for both the electrostatic and nonelectrostatic components [53,197] and the PB approach augmented by estimates of the hydrophobic contributions using the calculated surface area of the ligand [197,201].

Conformational averaging is widely used in free energy calculations of ligand binding [71,159]. What has been largely ignored is that, as in  $pK_a$  calculations, a proper LRA treatment requires averaging on both the charged (or polar) and nonpolar states of the ligand. The frequently neglected average on the nonpolar state (the second term of Eq. (9)) plays a crucial role in proteins because it reflects the effect of the protein preorganization [197]. The importance of this term in binding calculations is illustrated in an impressive way in studies of the fidelity of DNA polymerase [202–204] (See Table 1).

It should be mentioned here that despite the fact that the nonpolar term,  $\langle U_{\text{elect},\ell}^{\text{p}} \rangle_{\ell'}$ , can be of central importance in some cases of ligand binding, and is of fundamental importance in enzyme catalysis [205], there are cases where  $\langle U_{\text{elect},\ell}^{\text{p}} \rangle_{\ell'}$  is approximately zero [200] and can conveniently be neglected. The problem is to know when this approximation is valid.

One of the most serious problems in obtaining a converging result in calculations of binding free energies is that the binding process involves a change in the number of internal water molecules and can have a long relaxation time. To address this challenge we recently developed a FEP cycle in which the ligand is converted to water molecules in both the protein site and solution (see Fig. 8). Preliminary use of this treatment [206]

Table 1

Calculated relative binding free energies ( $\Delta \Delta G_{\text{bind}}$ ) for protein–DNA–substrate complexes with mismatched nucleotide pairs in T7 DNA polymerase<sup>a</sup>

Substrate	Template	$\Delta \Delta G_{\text{Q}}^{\text{ES}}$	$\Delta \Delta G_{\text{O}}^{\text{ES}}$	$\Delta \Delta G_{\text{bind},0}$	$\Delta \Delta G_{\text{bind}}$
dATP	T	0.0	0.0	0.0	0.0
	A <sup>b</sup>	1.0	1.4	1.0	3.4
	C <sup>b</sup>	3.1	1.8	0.4	5.3
	G	0.4	2.5	0.7	3.6
dTTP	A	0.0	0.0	0.0	0.0
	C <sup>b</sup>	0.5	2.7	1.0	4.2
	G	−0.3	4.8	−0.2	4.2
	T <sup>b</sup>	0.3	2.4	0.8	3.5
dGTP	C	0.0	0.0	0.0	0.0
	A <sup>b</sup>	5.3	3.7	0.5	9.5
	T <sup>b</sup>	4.7	7.7	0.6	13.0
dCTP	G	0.0	0.0	0.0	0.0
	C <sup>b</sup>	5.1	1.9	0.8	7.8
	A <sup>b</sup>	6.1	1.4	0.6	8.1
	T <sup>b</sup>	3.2	0.5	1.5	5.2

<sup>a</sup> Free energies (in kcal/mol) are given relative to the Watson–Crick pair with the correct dNTP template.  $\Delta \Delta G_{\text{Q}}^{\text{ES}}$  and  $\Delta \Delta G_{\text{O}}^{\text{ES}}$  denote the electrostatic components of  $\Delta \Delta G_{\text{bind}}$  calculated by averaging over trajectories for the charged and uncharged base of dNTP, respectively (Eq. (31)).  $\Delta \Delta G_{\text{bind},0}$  denotes the contribution from the binding of an uncharged ligand (Eq. (12)).

<sup>b</sup> Average of the results for ternary complexes with and without an extra water molecule inserted in the minor groove. Adapted from Florián et al. [203].

appeared to provide a clearer view of the nature of the water penetration contribution than was obtained previously by the PDL/D/S-LRA treatment [197]. The more microscopic results should increase our understanding of the nature of the LIE term, and should also significantly improve FEP and microscopic LRA calculations of binding energies (where the water penetration term plays a significant role).

Another fundamental problem is the evaluation of the binding entropy [197,207–211]. Unfortunately, it is very hard to evaluate entropic contributions and the corresponding errors are much larger than those for free energy calculations [212,213]. The harmonic or quasi-harmonic approximations that are frequently used to estimate this term [214,215] are unlikely to give quantitative results. A related estimate of the upper limit of the absolute entropy from the convergence matrix of the atomic fluctuations [216], which has been used in several studies (e.g., [217–219]) is also expected to provide only qualitative results [209]. Drawing on early ideas [220] and a related idea of Hermans and Wang [207], we have developed a variational restraint-release (RR) approach [208]. The RR approach is more general than Hermans' approach, since it is formulated in general Cartesian coordinates. More importantly, it recognizes that the RR free energy depends on the constraint coordinates, and it therefore minimizes the enthalpic contributions by searching for the lowest limit of the RR results. This approach has been used in several calculations of binding [197] and catalysis [221,222] and more systematic studies are underway.

Attempts to obtain more efficient ways to calculate binding entropies led Carlsson and Åqvist [209] to determine absolute translational and rotational entropies by evaluating the variance in the translational and rotational degrees of freedom during MD simulations. This approach gave encouraging results in a study of the entropic contribution of the binding of benzene to

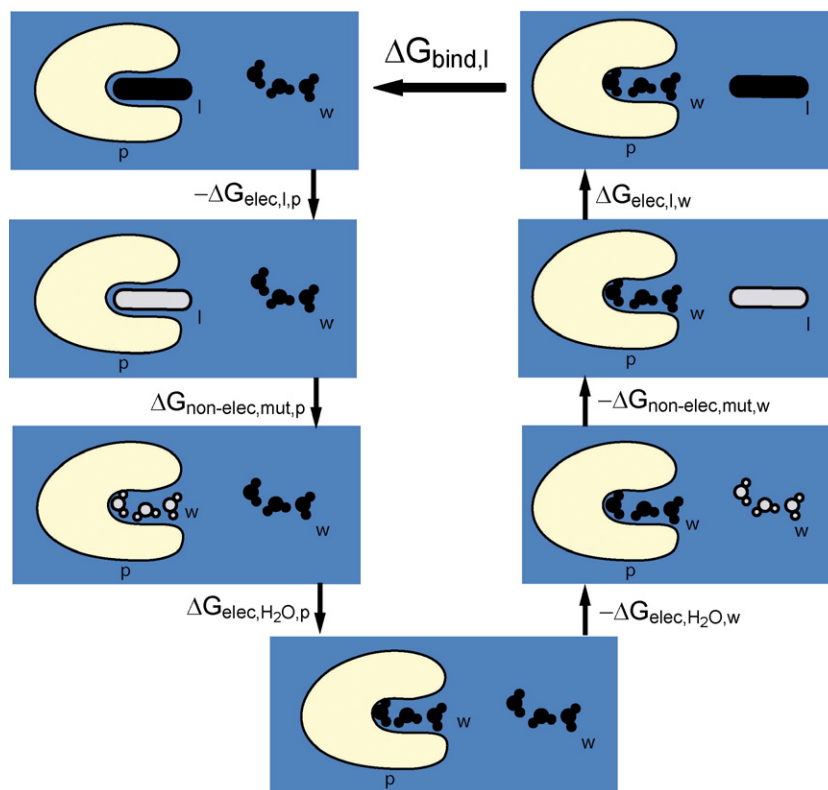


Fig. 8. A thermodynamic cycle that includes the water penetration effect associated with binding of a substrate (*I*) to a protein. The cycle involves mutation of the nonpolar form of the substrate to nonpolar water (*w*) molecules and then to polar water molecules. Polar and nonpolar forms are designated by black and light colors, respectively.

T4-lysozyme. However, the generality of the approach in cases with flexible ligands has not been demonstrated.

## 10. Enzyme catalysis and allosteric effects

Elucidating the catalytic power of enzymes is a subject of major practical and fundamental importance [136,223–225]. The introduction of combined quantum mechanical/molecular mechanics (QM/MM) computational models [11,223,225–231] provided a way to quantify the main factors that allow enzymes to reduce activation free energies. QM/MM studies, including those employing the empirical valence bond (EVB) method [136], have provided compelling support for the proposal [232] that electrostatic effects of preorganized active sites play a major role in stabilizing the transition states of enzymatic reactions [233], and there is growing acceptance of this view [234,235]. In fact, all the consistent calculations that actually reproduced the catalytic effect in a quantitative way have found that the major contribution comes from electrostatic effects. These findings are illustrated in Table 2 of [205]. Simulations that focus on electrostatic aspects of enzyme catalysis (i.e., on the difference between the electrostatic stabilization of the transition states of corresponding reactions in the enzyme and solution) appear to give much more accurate results than simulations that focus on quantum mechanical aspects of the problem but overlook a proper treatment of long-range electrostatic effects (see discussion in [236]). Some problems can be treated effectively even by PB approaches [237] without considering quantum mechanical

issues. Several studies have focused on the role of the diffusion step of enzyme catalysis [238,239], but the effects of enzymes in this step generally are much smaller than electrostatic effects in the actual chemical steps [240].

Interestingly, evaluations of activation free energies of enzymatic reactions appear to give more stable results than other types of electrostatic calculations such as binding free energies (see discussion in [241]). This advantage has been exploited for a long time in EVB studies [223] and is now being reflected in QM/MM studies [225,228,242].

Recent works have drawn renewed attention to effects of distant mutations on enzyme catalysis [243]. Although these effects have been viewed as a new paradigm for contributions of coupled vibrational modes to catalysis [243–245], they are basically allosteric effects. A change in interactions at one site causes a structural change that modifies the preorganization in the active site and thus affects catalysis (see discussion in [205]). Our analyses of allosteric effects [246–249] have identified the transfer of electrostatic effects as the most important factor, and as the best way of correlating the structural changes with the resulting catalytic effects. This point has been formulated recently in studies of the fidelity of DNA polymerase [250], where we introduced correlation matrixes based on energy coupling rather than on the less informative structural coupling [243,245].

A recent study [251] has attempted to deduce experimentally the strength of the electric field in the active sites of aldose reductase. This study provides an exciting new direction,

although the catalytic effect of aldose reductase is relatively small [252] and, thus, the electric field is smaller than in other enzymes. Furthermore, it is not entirely clear that the preorganization effect can be directly correlated with the macroscopic field.

Kraut et al. [253] have recently argued that electrostatic effects do not provide a major contribution to enzyme catalysis by ketosteroid isomerase (KSI). The authors found that the binding energies of phenolate ions to the oxyanion hole of the enzyme are not strongly correlated with the delocalization of the phenolate's charge (as estimated from NMR shifts). This weak correlation was assumed to provide an experimental tool for assessing the importance of electrostatic energies in enzyme catalysis. The finding of a very small change in binding energy for significant changes in delocalization was interpreted as evidence that electrostatic contributions do not play a major role in KSI and, presumably, in other enzymes as well. As in many other cases, however, there is a risk of confusing an interpretation of experimental facts with a unique energy-based analysis. Careful studies have shown that the catalytic effect of KSI is due almost entirely to electrostatic preorganization effects [254]. The experimental correlation described by Kraut et al. does not provide a way to estimate the actual electrostatic contribution or, for that matter, any other contribution. The authors simply postulated that the electrostatic contributions to both binding and catalysis must be correlated with the localization of the charge in the isolated phenolate, and tried to deduce the electrostatic contribution to catalysis from the localization. The most serious problem with this approach is that the catalytic cycle and the binding cycle are fundamentally very different; the catalytic cycle involves transfer of a negative charge from Asp 40 to the enolate oxygen, while binding involves movement of a negative charge from water to the protein active site. Calculations of the energetics of these processes (Warshel, A., Sharma, P. K., Chu, Z. T. and Åqvist, J., unpublished data), we found that the electrostatic contribution to binding is only about 2 kcal/mol as compared to about 10 kcal/mol in the catalytic process. The confusion here might have been due to the fact that the binding energy and the catalytic energy are of similar magnitudes (about 10 kcal/mol) and, thus, it possible to assume that both of them should reflect similar electrostatic contributions. However, most of the binding energy involves a nonpolar contribution, while the nonpolar contribution to catalysis is basically zero. Even if we overlook the difference between the cycle that leads to  $k_{\text{cat}}$  and the binding process and compare the binding of the enolate intermediate to the binding of the phenolates, we can see major differences between the two processes. That is, the electrostatic preorganization effect is, by far, larger in the case of the real substrate than in the case of the phenolates. This reflects the fact that the preorganization effect depends on the orientation of the nonpolar from the ligand (the second term in Eq. 9) relative to the oxyanion hole, as well as on the polarization of the oxyanion hole in the absence of a charge on the ligand. Apparently, when the phenolate is in the nonpolar state, it can easily move out of the correct orientation.

Another problem is that a more localized charge on the phenolate will also lead to greater electrostatic stabilization (solvation) in the reference solvent, so that the net effect on catalysis (i.e., on the ratio of the enzymatic and nonenzymatic

reactions) is smaller than one might anticipate. Thus, the attempt to deduce the electrostatic effect from the  $\text{p}K_{\text{a}}$  of the phenolates is very problematic unless it involves careful calculations of the actual electrostatic contributions.

## 11. Ion Pairs

Ion pairs play major roles in many biological systems. These include the “salt bridges” that control the Bohr effect in hemoglobin [255], ion-pair type transition states [136], and ion pairs that mediate protein–protein interactions (Section 12), contribute to protein stability (Section 13), or participate in photobiological processes [256,257]. Reliable analysis of the energetics of ion pairs in proteins presents a major challenge and has engendered significant conceptual confusions (see discussions in [10,12]). The most common point of confusion is the intuitive assumption that nonpolar environments stabilize ion pairs (see the analysis in [256,258]). Examples of this confusion are found even in recent studies [259] and in most desolvation models of enzyme catalysis [260–262], which are based on the assumption that enzymes destabilize reaction ground states by placing the substrates in nonpolar environments. As has been demonstrated elsewhere [136,241], enzymes do not provide nonpolar active sites for ion-pair type ground states: they provide very polar environments that stabilize the transition states. In general, ion pairs are not stable in nonpolar sites in proteins. Most ion pairs in proteins are located on the surface, and those that are located in protein interiors are always surrounded by polar environments [136]. Forcing an ion pair between amino acids to be in a nonpolar environment usually results in proton transfer from the base to the acid, converting the pair to its nonpolar form.

The energetics of ion pairs in proteins has been studied by both microscopic FEP calculations [263,264] and semimacroscopic calculations [19,42,70,265,266]. However, there are very few systematic validation studies. An instructive example is the work of Hendsch and Tidor, who used a PB approach with a low value of  $\epsilon_{\text{p}}$  to study the energetics of forming ion pairs in T4 lysozyme [267]. The calculated energies for the processes  $\text{Asp70}^0 \cdots \text{His31}^+ \rightarrow \text{Asp70}^- \cdots \text{His31}^+$  and  $\text{Asp70}^- \cdots \text{His31}^0 \rightarrow \text{Asp70}^- \cdots \text{His31}^+$  were  $-0.69$  and  $-0.77$  kcal/mol, respectively. These values can be compared to the observed energies of  $-4.7$  and  $-1.9$  kcal/mol. A reanalysis using the PDL/D/S-LRA model gave values of  $-4.7$  and  $-2.2$  kcal/mol, which agree much better with experiment [19]. Similarly, Hendsch and Tidor's estimate of 10 kcal/mol destabilization of the Glu11–Arg45 ion pair in T4 lysozyme seems to be a significant overestimate relative to the result of  $\sim 3$  kcal/mol obtained by the PDL/D/S-LRA approach. It is significant that the  $\text{Asp70}^- \cdots \text{His31}^+$  ion pair apparently does not destabilize the protein. Schutz and Warshel [19] found the energy of moving this ion pair from infinite separation in water to the protein site (relative to the corresponding energy for the neutral residues) to be close to zero, whereas Hendsch and Tidor's [267] value was 3.46 kcal/mol. The difference between the two studies can be traced in part to the estimate of the stabilizing effect of the protein permanent dipoles ( $\Delta U_{\text{Q}_{\text{H}}}$ ). The PDL/D/S-LRA calculation gave a  $\Delta U_{\text{Q}_{\text{H}}}$  of approximately

–5 kcal/mol [19], whereas the PB treatment [267] gave  $\sim -0.26$  kcal/mol. The smaller value found in the PB calculations could reflect the use of an approach that does not allow polar groups to reorient in response to the charges of the ion pair. It is the stabilizing effect of the protein polar groups that plays a crucial role in stabilizing ion pairs in proteins. Clearly, estimates of the energetics of ion pairs depend crucially on the dielectric constant used, and models that do not consider the protein relaxation explicitly must use a larger  $\epsilon_p$  than the PDL/D/S-LRA model.

There is a need for more systematic validation studies that consider internal ion pairs with well-defined structure and energy. The statistical analyses that have been reported so far [268], though instructive, are likely to involve problems similar to those mentioned in Section 5, since they consider mainly surface groups, a non-discriminative data base, rather than ion pairs in protein interiors.

## 12. Protein–protein interactions

Protein–protein interactions play a crucial role in many biological systems, including signal transduction [269], energy transduction [270], assembly processes [22] and electron transport [271,272]. Here again, electrostatic effects appear to be a major factor in determining the nature and strength of the interaction between protein surfaces [273–277].

Calculations of protein–protein interactions are very challenging because of the large surfaces involved and the large structural changes that can occur upon binding [116,278,279]. Considering the protein reorganization upon binding is particularly difficult and an LRA study that tried to accomplish this task for the Ras/RAF system [116] did not obtain quantitative results. However, a much simpler approach, in which charge–charge interactions were evaluated by Eq. (16), gave encouraging results for the effect of mutations on the binding energy between the two proteins [116].

Recent PB studies of binding of the proteins by barnase and barstar also have met with some success, but indicate that the results are very sensitive to the dielectric model used [276,277]. Some progress has also been reported in studies of the effect of mutations on protein–protein interactions using the LIE approach, which, however, requires different parameters from those used in binding studies [200].

## 13. Folding and stability

Studies of protein folding by simulation approaches date back to the introduction of a simplified folding model in 1975 [280], which showed that the folding problem is much simpler than previously thought. The simplified folding model and the somewhat less physical model developed by Go [281], which are sometimes classified as off-lattice and on-lattice models, respectively, paved the way to major advances in understanding the free energy landscape of protein folding [282–285]. Further progress has been achieved by all-atom simulations of peptides and small proteins [286–290], by MD simulations with united-residue models [291,292], and by using additional structural

information such as the orientation dependence of hydrogen bonds [293]. Some of these simulations involve explicit solvent models, but most use implicit solvation models ranging from GB type models [286] to the Langevin dipole model [288]. Interesting insights have been provided by the idea of using a simplified folding model as a reference potential for all-atom free energy simulation [288], but the full potential of this approach has not yet been exploited. Another promising direction is the use of distributed computing resources [294].

At present, it seems that simplified folding models can describe the average behavior of all-atom models quite well, although more systematic studies are needed. The use of implicit solvent models also looks promising but here again there is a clear need for detailed validation studies focusing on measured electrostatic energies.

Despite the impressive progress in studies of protein folding, we still lack a clear understanding of the contributions of electrostatic contributions to thermal stability. Experimental studies of mesophilic, thermophilic, and hyperthermophilic proteins have provided an excellent benchmark for studies in this area [295,296]. In general, the number of ionizable residues increases in hyperthermophiles, indicating that charged residues can be considered as a stabilizing factor. However, some continuum studies have suggested that charged and polar groups lead to destabilization [267] [297]. Hendsch and Tidor [267] concluded that internal salt bridges tend to destabilize proteins, although as discussed in Section 11, this study did not reproduce the relevant observed energies. Other studies [298–301] appear to support the idea that charged residues can help to optimize protein stability.

The difficulty in reaching clear conclusions on the role of electrostatic interactions in protein stability is that we have a competition between desolvation penalties, stabilization by local protein dipoles, and charge–charge interactions. In the original TK model of a hydrophobic protein [5], both isolated ions and ion pairs become unstable in the “protein” interior [10]. However, the situation is much more complex in real proteins, where charges are stabilized by polar groups. Here the balance between charge–charge interactions and self-energy can depend drastically on the assumed  $\epsilon_p$ . As stated in previous sections, it seems to us that different values of  $\epsilon_p$  should be used for charge–charge interactions and self-energies. The above point can be clarified by writing the contribution of the ionizable residues to the folding energy as

$$\begin{aligned} \Delta G_{\text{fold}}^{\text{elec}} &= \Delta G_f^{\text{elec}} - \Delta G_{\text{uf}}^{\text{elec}} = \\ &- 2.3RT \sum_i Q_i^{(f)} \left( \text{p}K_{i,\text{int}}^p(\epsilon_p) - \text{pH} \right) \\ &+ 166 \sum_{i>j} \frac{Q_i^{(f)} Q_j^{(f)}}{r_{ij}^{(f)} \epsilon_{\text{eff}}(r_{ij}^{(f)})} - 2.3RT \sum_i Q_i^{(\text{uf})} \left( \text{p}K_{a,i}^w - \text{pH} \right) \\ &- 166 \sum_{i>j} \frac{Q_i^{(\text{uf})} Q_j^{(\text{uf})}}{80r_{ij}^{(\text{uf})}}, \end{aligned} \quad (33)$$

where f and uf designate, respectively, the folded and unfolded form of the protein, and  $Q_i$  is the charge of group  $i$ . This

expression is based on our previous description of the electrostatic free energies of ionization states in proteins [302] and on the simplified approximation that the charges are fully solvated by water ( $\epsilon \approx 80$ ) in the unfolded state. If we assume that the same groups are ionized in the folded state, Eq. (33) simplifies to

$$\Delta G_{\text{fold}}^{\text{elec}} \approx -2.3RT \sum_i Q_i \left( \text{p}K_{i,\text{int}}^{\text{p}}(\epsilon_p) - \text{p}K_{i,\text{w}}^{\text{w}} \right) + 166 \sum_{i>j} Q_i Q_j \left[ \frac{1}{r_{ij}^{(f)} \epsilon_{\text{eff}}^{(f)}(r_j)} - \frac{1}{80r_{ij}^{(uf)}} \right]. \quad (34)$$

The first term in Eq. (34) represents the change of self-energy upon moving a charge from water to its site in the protein (this term depends on  $\epsilon_p$ ), and the second term represents the effect of charge–charge interactions. In general the effective dielectric constant that enters into the first term and the  $\epsilon_{ij}$  of the second term are quite different, and this makes the analysis complicated. Schutz and Warshel (unpublished results) used this treatment to evaluate the relative folding energies of homologous cold-shock proteins from the mesophilic bacterium *Bacillus subtilis* [303] and the thermophilic bacterium *Bacillus caldolyticus*. They were able to reproduce the increased stability of the thermophilic protein with  $\epsilon_p=8$  and  $\epsilon_{\text{eff}} \approx 20$ . The same problem has been addressed by Brooks and coworkers [304], who examined the electrostatic contribution to the enhanced stability of thermophilic proteins with respect to their mesophilic homologues. These authors found that the calculated  $\bar{\epsilon}$  increases from mesophiles to hypothermophiles, probably reflecting the different charge distribution. They also explored the folding energy using a GB model. It was found that a relatively large  $\epsilon_{\text{eff}}$  (called  $\epsilon_p$  in Ref. [304]) is needed in order to reproduce the observed trend. Since this treatment used the same  $\epsilon_{\text{eff}}$  for both the self-energy and the charge–charge terms, the conclusion might be still somewhat problematic. At any rate, it seems to us analysis based on Eq. (34) or the approach of Ref. [304] must be subjected to careful validation studies focusing particularly on reproduction of the observed  $\text{p}K_{\text{a}}$ s of the proteins under consideration.

#### 14. Ion and proton channels

The control of ion permeation by transmembrane channels underlies many important biological functions [305]. Understanding the control of ion selectivity by ion channels is basically a problem in protein electrostatics that turns out to be a truly challenging task [306–308]. The primary problem is the evaluation of the free energy profile for transferring a given ion from water to a particular position in the channel. It is also essential to evaluate the interaction between ions in the channel if the ion current involves a multi-ion process [155]. Early studies of ion channels focused on the energetics of ions in the gramicidin channel [46,309]. The solution of the structure of the KcsA potassium channel [310] provided a model for real biological channels and a major challenge for simulation approaches. Some early studies (e.g., [311,312]) provided se-

vere overestimates of the barriers for ion transport. The first realistic results were obtained by Åqvist and Luzhkov [313], who carried out FEP calculations using the LRF long-range treatment and SCSSA boundary conditions. Microscopic attempts to obtain the selectivity difference between  $\text{K}^+$  and  $\text{Na}^+$  were also reported [154]. However, these studies did not evaluate the activation barriers for the two different ions and thus could not provide the difference between the corresponding currents. Furthermore, attempts to evaluate the PMF for ion penetration have not succeeded in reproducing the actual PMF for moving the ions from water to the channel (see discussion in [155]).

The semimacroscopic PDL/D/S-LRA approach provides a promising alternative that appears to be effective in capturing the energetics of ion transport through the KcsA channel. Calculations using this approach reproduced the  $\text{K}^+/\text{Na}^+$  selectivity and led to estimates of the activation barriers that accounted for the difference between the  $\text{Na}^+$  and  $\text{K}^+$  currents [314]. The LRA treatment was essential in order to capture the change in the protein (channel) structure when the ion changes from  $\text{K}^+$  to  $\text{Na}^+$ , which is difficult to treat by any other available method. It is important to note that modeling the ion current by Langevin Dynamics or related approaches requires a very fast evaluation of the electrostatic energies at various configurations of the moving ions. The PDL/D/S-LRA approach with a distance-dependent dielectric constant (Eq. (16)) proved to be useful for this [155].

Cymes et al. [315] have introduced protonating groups one at a time along the channel of the nicotinic-acetylcholine receptor and have evaluated the  $\text{p}K_{\text{a}}$ 's of these groups. This approach, coupled with proper structural and computational analysis, should provide a way to validate electrostatic models for ion channels.

The discovery of aquaporins and their remarkable role in conducting water molecules through cell membranes has attracted major interest [316–318]. One of the main questions that this discovery raises is how the aquaporin channel blocks movement of protons across the membrane [319–329]. Early studies [320,324] suggested that this blockade depends on water orientational effects that disrupt the Grothuss mechanism of proton diffusion [330–332]. Recent work, however, supports the view that the blockage is due to an electrostatic barrier [321,323,325,326,329,333]. This conclusion is in line with the earlier general proposal that proton transport in proteins is controlled by electrostatic barriers [302,334]. This point is illustrated in Fig. 9, which shows schematically that the energy invested in orienting the water molecules is much smaller than the energy required to move the positive charge of the proton through the channel.

Although the importance of an electrostatic barrier to proton movement now appears to be generally accepted, the origin and magnitude of this barrier remain controversial. Some workers have attributed the barrier to special structural elements [321,323] and, in particular, to a so-called NPA motif [319,323,329,333], ionized residues [329], and/or helix dipoles [320,325,326]. Burykin and Warshel concluded that the barrier comes mainly from the cost of desolvation as the charge moves from bulk water to the center of the channel [327,328]. These

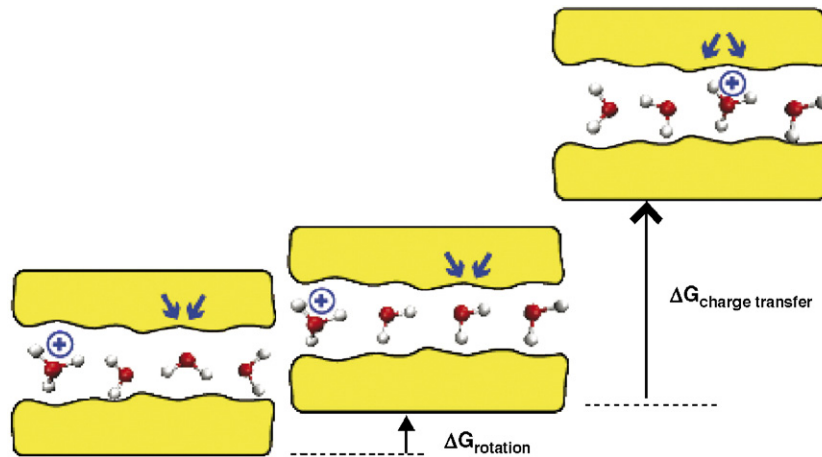


Fig. 9. An illustration of the idea that the barrier to proton movements in aquaporin is not due to the orientation of the water molecules, but rather to an electrostatic barrier for the transfer of charge. The figure divides the overall process of proton transfer to the center of the channel into two steps: first rotation of the water molecules and then transferring the proton charge against the electrostatic barrier. The figure ignores the fact that a complete orientation of the water molecules is not needed [346,347].

different views are shown schematically in Fig. 10, which is a modification of an illustration presented by de Groot and Grubmüller [325].

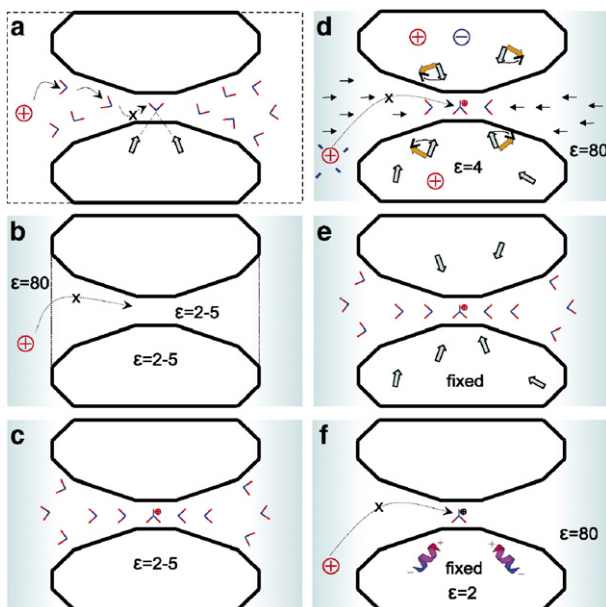


Fig. 10. A schematic depiction of various proposals for the origin of the barrier to proton transport in aquaporin. (a) The view that the barrier is due to an orientation constraint imposed on the water molecules by the NPA motif [320,324]. (b) A model in which the channel is described by a low dielectric constant ( $\epsilon=2.5$ ) [325]. (This model represents a misunderstanding of the proposal of Burykin and Warshel [327,328], who emphasized that the overall effect of the channel corresponds to an effective dielectric constant of about 7.) (c) The same as (b) but with the more reasonable assumption that the pore is represented by a high dielectric or by a simplified solvent model. (d) The Burykin–Warshel model, which considers all the electrostatic elements in the channel in a consistent way and examines the overall effect in substituting the solvation of the charge by the bulk water. (e) The same as (d) but with fixed protein dipoles (i.e., with the protein dipoles prevented from rearranging during the charging process) [323,326]. (f) The idea that the electrostatic barrier is due to helix dipoles [325,326]. From Kato et al. [335].

A recent study [335] examined the origin of the barrier for proton transport in aquaporin by semimacroscopic and microscopic calculations and explored the effect of different factors, emphasizing the reliability of the calculations and the problems with alternative approaches. As shown in Fig. 11, the calculated effects of the NPA motif is much smaller than would be concluded from semimacroscopic calculations that do not use the LRA approach and that hold the protein fixed when the charges of the NPA residues are removed. Similar results were obtained for the mutation of the helix dipoles (see below). Other calculations illustrated the problems with microscopic PMF calculations that attempt to determine the effect of the mutations but neglect the work of moving the ion from the bulk water into the channel. Overall, it seems clear that the barrier for proton transfer in proteins is determined by the overwhelming electrostatic barrier to desolvation of the charge. This barrier

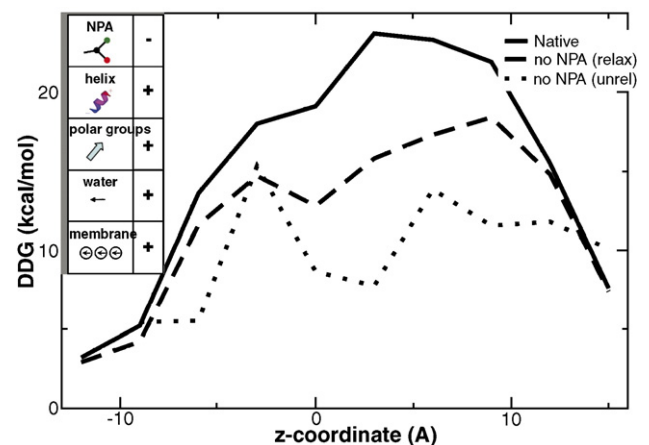


Fig. 11. The PDL/D-S-LRA estimate of the effect of the NPA residues on the electrostatic barrier. The figure provides both the results for mutations of the NPA residues and the inconsistent estimates of the effect of the NPA motif obtained by the calculations using  $\epsilon_p=4$  without relaxations of the proteins. The fact that the NPA region is mutated is designated by the minus sign in the corresponding box. Taken from Kato et al. [335].

can be modulated by specific electrostatic interactions with the protein, but can be eliminated only when the sum of the electrostatic contributions from the protein permanent dipoles, induced dipoles and the charges is as favorable as solvation of the ion in water.

### 15. Helix macrodipoles versus localized molecular dipoles

The idea that the macroscopic dipoles of  $\alpha$ -helices can contribute to the electrostatic energies ligand binding and other processes in proteins [336,337] is very appealing. There is, however, a tendency to overestimate the importance of these macrodipoles relative to the effects of the microscopic dipoles due to individual hydrogen bonds, carbonyl groups and other polar groups. Most estimates of the magnitudes of helix-dipole effects [337–341] have used unrealistically low values for the pertinent dielectric constant, and few investigators have attempted to verify their estimate by using the same model in calculations of relevant observables such as  $pK_a$  shifts or effects on enzyme catalysis. The first quantitative estimate of the effect of the helix dipole [342] established that the actual effect can be attributed almost entirely to the first few microscopic dipoles at the end of the helix, rather than to the macrodipole of the entire helix. Contributions from more distant residues are attenuated strongly by dielectric screening. It was predicted that neutralizing the end of the helix by an

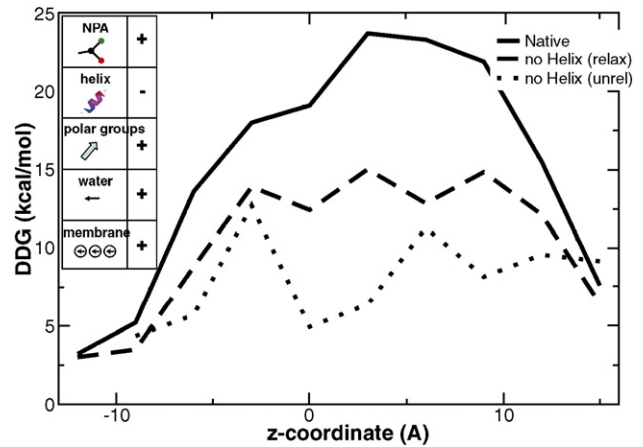


Fig. 13. The effect of the helix macrodipole on the electrostatic barrier. The figure depicts the consistent PDL/S-LRA results as well as the inconsistent unrelaxed results. Taken from Ref. [335].

opposing charge would have only a small effect, which was confirmed experimentally [343].

Recent studies of the KcsA  $K^+$  channel provide an illustration of the need for a proper treatment of helix dipoles. Using PB calculations with  $\epsilon_p=2$ , Roux and MacKinnon [344] obtained an extremely large effect of helix dipoles ( $\sim -20$  kcal/mol) on the stabilization of a  $K^+$  ion in the central cavity.

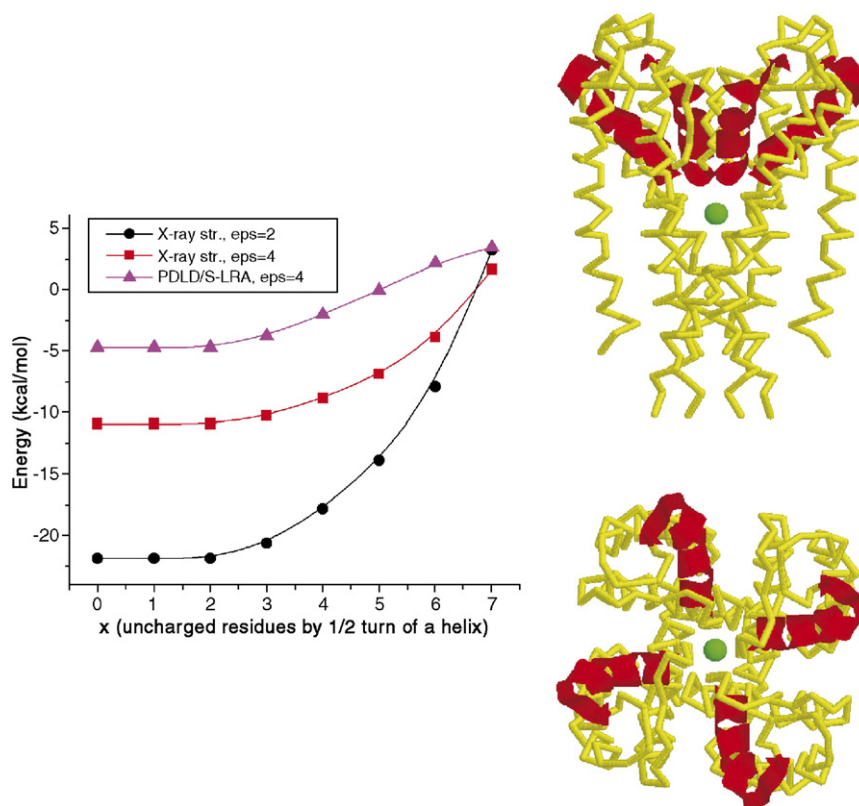


Fig. 12. The effect of the helix dipoles of the KcsA ion channel on a  $K^+$  ion in the central cavity. In the structural drawing on the right,  $K^+$  is shown in green and the four  $\alpha$ -helices that point toward the ion are represented by red ribbons. The graph on the left shows the contribution of the backbone atoms in the four helices as a function of the dielectric treatment used. Using  $\epsilon_p=2$  overestimates the contribution of the macrodipoles relative to the more realistic estimate obtained by the PDL/S-LRA treatment. The graph also shows that removing the charges of up to three residues at the distal ends of the helices has little effect on the calculated energies.

Burykin et al. [314], using an LRA procedure in the framework of the PDL/S-LRA approach, obtained a much smaller effect (see Fig. 12). The former procedure appears to overestimate the effect of the helix dipole by a factor of about 3. A similar problem occurs in aquaporin, where it has been suggested [325,326] that the helix dipole is responsible for the barrier to proton transfer (see Fig. 10f). A careful analysis (see Fig. 13) indicated that the helix macrodipole (or more precisely, its end) contributes only about 4 kcal/mol to the overall barrier [335]. A recent experimental attempt to cancel the effect of the macrodipole in KcsA by introducing positively charged residues supports this conclusion [345].

## 16. Concluding remarks

Almost all biological processes are controlled or modulated by electrostatic effects, and the key for almost any quantitative structure–function correlation in proteins is the ability to perform accurate electrostatic calculations. However, the need for discriminative validation studies has not received the attention it warrants. Focusing on trivial properties of surface groups can lead to an overly positive impression of the reliability of a model and can obscure the relative merits of different approaches. There also is a worrisome tendency to validate new implicit models by their ability to reproduce PB results. For example, GB calculations sometimes are verified by comparing them to the corresponding PB calculations. This assumes that the PB results represent the correct electrostatic energies, overlooking the fact that these calculated energies depend critically on an assumed dielectric constant. Consistent validations and developments of reliable models should involve comparisons to relevant experimental results in meaningful test cases. Although verification of semimacroscopic models might also involve a comparison to microscopic results, at present many microscopic calculations do not reach reasonable convergence. In this respect, an appreciation of the importance of long-range effects, proper boundary conditions, and convergence issues should help to increase the accuracy of microscopic models. The continuing increase in computational resources also should contribute toward this goal.

Our critical discussion of various semimacroscopic approaches does not at all mean that such approaches are not useful. The PB and GB models, for example, provide excellent models for the effect of the solvent around the protein. And as long as the difficulties of obtaining reliable results by microscopic approaches persist, one must resort to semimacroscopic approaches. Semimacroscopic approaches are also essential in problems such as the protein-folding problem, where the need to sample vast amounts of conformational space imposes a demand for fast evaluation of the relevant electrostatic energies. The results obtained by semimacroscopic models should become increasingly accurate as we obtain a better understanding of dielectric screening in proteins. This can be considered more as progress in developing the correct scaling in advanced implicit models, rather than as a search for the non-existent universal dielectric “constant” of proteins.

## Acknowledgements

This work was supported by the NIH grants GM40283, GM24492 and R37GM21422 and NSF grant MCB-0003872.

## References

- [1] M.F. Perutz, Electrostatic effects in proteins, *Science* 201 (1978) 1187–1191.
- [2] A. Warshel, Electrostatic basis of structure–function correlation in proteins, *Acc. Chem. Res.* 14 (1981) 284–290.
- [3] K.A. Sharp, B. Honig, Electrostatic interactions in macromolecules: theory and applications, *Annu. Rev. Biophys. Biophys. Chem.* 19 (1990) 301–332.
- [4] K. Linderstrom-Lang, The ionization of proteins, *C. R. Trav. Lab. Carlsberg* 15 (1924) 29.
- [5] C. Tanford, J.G. Kirkwood, Theory of protein titration curves. I. General equations for impenetrable spheres, *J. Am. Chem. Soc.* 79 (1957) 5333.
- [6] H. Nakamura, Roles of electrostatic interaction in proteins, *Q. Rev. Biophys.* 29 (1996) 1–90.
- [7] M.E. Davis, J.A. McCammon, Electrostatics in biomolecular structure and dynamics, *Chem. Rev.* 90 (1990) 509–521.
- [8] A. Warshel, A. Papazyan, Electrostatic effects in macromolecules: fundamental concepts and practical modeling, *Curr. Opin. Struct. Biol.* 8 (1998) 211–217.
- [9] T. Simonson, Electrostatics and dynamics of proteins, *Rep. Prog. Phys.* 66 (2003) 737–787.
- [10] A. Warshel, S.T. Russell, A.K. Churg, Macroscopic models for studies of electrostatic interactions in proteins: limitations and applicability, *Proc. Natl. Acad. Sci. U. S. A.* 81 (1984) 4785–4789.
- [11] A. Warshel, M. Levitt, Theoretical studies of enzymic reactions: dielectric, electrostatic and steric stabilization of the carbonium ion in the reaction of lysozyme, *J. Mol. Biol.* 103 (1976) 227–249.
- [12] A. Warshel, S.T. Russell, Calculations of electrostatic interactions in biological systems and in solutions, *Q. Rev. Biophys.* 17 (1984) 283–421.
- [13] A. Warshel, J. Åqvist, Electrostatic energy and macromolecular function, *Ann. Rev. Biophys. Chem.* 20 (1991) 267–298.
- [14] W.W. Parson, A. Warshel, Calculations of electrostatic energies in proteins using microscopic, semimicroscopic and macroscopic models and free-energy perturbation approaches, in: J. Matysik, T.J. Aartsma (Eds.), *Biophysical Techniques in Photosynthesis Research II*, Springer, Dordrecht, 2006.
- [15] S. Braun-Sand, A. Warshel, Electrostatics of proteins: principles, models and applications, in: J. Buchner, T. Kiefhaber (Eds.), *Protein Folding Handbook. Part I*, Wiley-VCH, Weinheim, 2005.
- [16] J.D. Jackson, *Classical Electrodynamics*, 3rd ed. John Wiley and Sons, Inc., New York, 1999.
- [17] W.H. Orttung, Polarizability of density of inert-gas atom pairs. I, *J. Phys. Chem.* 89 (1985) 3011–3016.
- [18] J. Warwicker, H.C. Watson, Calculation of the electric potential in the active site cleft due to alpha-helix dipoles, *J. Mol. Biol.* 157 (1982) 671–679.
- [19] C.N. Schutz, A. Warshel, What are the dielectric ‘constants’ of proteins and how to validate electrostatic models, *Proteins: Struct. Funct. Genet.* 44 (2001) 400–417.
- [20] A. Warshel, What about protein polarity? *Nature* 333 (1987) 15–18.
- [21] J.B. Matthew, P.C. Weber, F.R. Salemme, F.M. Richards, Electrostatic orientation during electron-transfer between flavodoxin and cytochrome-C, *Nature* 301 (1983) 169–171.
- [22] A.C. Bloomer, J.N. Champness, G. Bricogne, R. Staden, A. Klug, Protein disk of tobacco mosaic-virus at 2.8-Å resolution showing interactions within and between subunits, *Nature* 276 (1978) 362–368.
- [23] C.A. Vernon, Mechanisms of hydrolysis of glycosides and their relevance to enzyme-catalyzed reactions, *Proc. R. Soc., Ser. B* 167 (1967) 389–401.
- [24] H. Dufner, S.M. Kast, J. Brickmann, M. Schlenkrich, Ewald summation versus direct summation of shifted-force potentials for the calculation of

- electrostatic interactions in solids—A quantitative study, *J. Comp. Chem.* 18 (1997) 660–675.
- [25] A. Warshel, Z.T. Chu, Calculations of solvation free energies in chemistry and biology, in: C.J. Cramer, D.G. Truhlar (Eds.), *ACS Symposium Series: Structure and Reactivity in Aqueous Solution. Characterization of Chemical and Biological Systems*, ACS, Washington, DC, 1994, pp. 72–93.
- [26] F. Figueirido, G.S. Del Buono, R.M. Levy, On the finite size corrections to the free energy of ionic hydration, *J. Phys. Chem., B* 101 (1997) 5622–5623.
- [27] G. Hummer, L.R. Pratt, A.E. Garcia, Free energy of ionic hydration, *J. Phys. Chem.* 100 (1996) 1206–1215.
- [28] Y.Y. Sham, A. Warshel, The surface constrained all atom model provides size independent results in calculations of hydration free energies, *J. Chem. Phys.* 109 (1998) 7940–7944.
- [29] M.A. Kastenholtz, P.H. Hünenberger, Computation of methodology-independent ionic solvation free energies from molecular simulations: I. The electrostatic potential in molecular liquids, *J. Chem. Phys.* 124 (2006) 124106/1–124106–27.
- [30] Y.N. Vorobjev, J. Hermans, A critical analysis of methods of calculation of a potential in simulated polar liquids: strong arguments in favor of “Molecule-Based” summation and of vacuum boundary conditions in ewald summation, *J. Phys. Chem., B* 103 (1999) 10234–10242.
- [31] M.A. Villarreal, G.G. Montich, On the Ewald artifacts in computer simulations. The case of the octaalanine peptide with charged termini, *J. Biomol. Struct. Dyn.* 23 (2005) 135.
- [32] J. Aqvist, T. Hansson, Analysis of electrostatic potential truncation schemes in simulations of polar solvents, *J. Phys. Chem., B* 102 (1998) 3837–3840.
- [33] Y.Y. Sham, A. Warshel, The surface constrained all atom model provides size independent results in calculations of hydration free energies, *J. Chem. Phys.* 109 (1998) 7940–7944.
- [34] J. Aqvist, Comment on transferability of ion models, *J. Phys. Chem.* 98 (1994) 8253–8255.
- [35] S. Kuwajima, A. Warshel, The extended ewald method: a general treatment of long-range electrostatic interactions in microscopic simulations, *J. Chem. Phys.* 89 (1988) 3751–3759.
- [36] F.S. Lee, A. Warshel, A local reaction field method for fast evaluation of long-range electrostatic interactions in molecular simulations, *J. Chem. Phys.* 97 (1992) 3100–3107.
- [37] A. Warshel, Calculations of chemical processes in solutions, *J. Phys. Chem.* 83 (1979) 1640–1650.
- [38] S.A. Adelman, *Adv. Chem. Phys.* 53 (1983) 61.
- [39] A. Brunger, C.L.B. III, M. Karplus, *Chem. Phys. Lett.* 105 (1984) 495.
- [40] G. King, A. Warshel, A surface constrained all-atom solvent model for effective simulations of polar solutions, *J. Chem. Phys.* 91 (1989) 3647–3661.
- [41] J.G. Kirkwood, Theory of solutions of molecules containing widely separated charges with special application to zwitterions, *J. Chem. Phys.* 2 (1934) 351.
- [42] F.S. Lee, Z.T. Chu, A. Warshel, Microscopic and semimicroscopic calculations of electrostatic energies in proteins by the POLARIS and ENZYMI programs, *J. Comp. Chem.* 14 (1993) 161–185.
- [43] H. Alper, R.M. Levy, Dielectric and thermodynamic response of generalized reaction field model for liquid state simulations, *J. Chem. Phys.* 99 (1993) 9847.
- [44] S.T. Russell, A. Warshel, Calculations of electrostatic energies in proteins; the energetics of ionized groups in bovine pancreatic trypsin inhibitor, *J. Mol. Biol.* 185 (1985) 389–404.
- [45] R.G. Alden, W.W. Parson, Z.T. Chu, A. Warshel, Calculations of electrostatic energies in photosynthetic reaction centers, *J. Am. Chem. Soc.* 117 (1995) 12284–12298.
- [46] J. Åqvist, A. Warshel, Energetics of ion permeation through membrane channels. Solvation of Na<sup>+</sup> by Gramicidin A, *Biophys. J.* 56 (1989) 171–182.
- [47] B. Roux, M. Karplus, Ion transport in the gramicidin channel: free energy of the solvated right-handed dimer in a model membrane, *J. Am. Chem. Soc.* 115 (1993) 3250–3260.
- [48] H.A. Stern, F. Rittner, B.J. Berne, R.A. Friesner, Combined fluctuating charge and polarizable dipole models: application to a five-site water potential function, *J. Chem. Phys.* 115 (2001) 2237–2251.
- [49] P.Y. Ren, J.W. Ponder, Consistent treatment of inter- and intramolecular polarization in molecular mechanics calculations, *J. Comp. Chem.* 23 (2002) 1497–1506.
- [50] A. Warshel, F. Sussman, G. King, Free energy of charges in solvated proteins: microscopic calculations using a reversible charging process, *Biochemistry* 25 (1986) 8368–8372.
- [51] P. Kollman, Free energy calculations: applications to chemical and biochemical phenomena, *Chem. Rev.* 93 (1993) 2395–2417.
- [52] A. Warshel, Dynamics of reactions in polar solvents. semiclassical trajectory studies of electron-transfer and proton-transfer reactions, *J. Phys. Chem.* 86 (1982) 2218–2224.
- [53] F.S. Lee, Z.T. Chu, M.B. Bolger, A. Warshel, Calculations of antibody-antigen interactions: microscopic and semi-microscopic evaluation of the free energies of binding of phosphorylcholine analogs to McPC603, *Prot. Eng.* 5 (1992) 215–228.
- [54] Y.Y. Sham, Z.T. Chu, A. Warshel, Consistent calculations of pK<sub>a</sub>'s of ionizable residues in proteins: semi-microscopic and macroscopic approaches, *J. Phys. Chem., B* 101 (1997) 4458–4472.
- [55] G.S. Del Buono, F.E. Figueirido, R.M. Levy, Intrinsic pK<sub>a</sub>s of ionizable residues in proteins: an explicit solvent calculation for lysozyme, *Protein: Struct. Funct. Genet.* 20 (1994) 85–97.
- [56] M. Saito, Molecular dynamics free-energy study of a protein in solution with all degrees of freedom and long-range Coulomb interactions, *J. Phys. Chem.* 99 (1995) 17043–17048.
- [57] M. Kato, A. Warshel, Through the channel and around the channel: validating and comparing microscopic approaches for the evaluation of free energy profiles for ion penetration through ion channels, *J. Phys. Chem. B* 109 (2005) 19516–19522.
- [58] A.M. Ferrenberg, R.H. Swendsen, Optimized Monte Carlo data analysis, *Phys. Rev. Lett.* 63 (1989) 1195–1198.
- [59] C. Jarzynski, Nonequilibrium equality for free energy differences, *Phys. Rev. Lett.* 78 (1997) 2690–2693.
- [60] I. Andricioaei, A.R. Dinner, M. Karplus, Self-guided enhanced sampling methods for thermodynamic averages, *J. Chem. Phys.* 118 (2003) 1074–1084.
- [61] B. Roux, The calculation of the potential of mean force using computer simulations, *Comput. Phys. Commun.* 91 (1995) 275–282.
- [62] E.M. Purcell, *Electricity and Magnetism*, McGraw-Hill Book Company, 1965.
- [63] Y. Liu, T. Ichiye, The static dielectric-constant of the soft sticky dipole model of liquid water—Monte Carlo simulation, *Chem. Phys. Lett.* 256 (1996) 334–340.
- [64] R.D. Coalson, A. Duncan, Statistical mechanics of a multipolar gas: a lattice field theory approach, *J. Phys. Chem.* 100 (1996) 2612–2620.
- [65] A. Papazyan, A. Warshel, Continuum and dipole-lattice models of solvation, *J. Phys. Chem.* 101 (1997) 11254–11264.
- [66] A. Papazyan, A. Warshel, Effect of solvent discreteness on solvation, *J. Phys. Chem., B* 102 (1998) 5248–5357.
- [67] N.K. Rogers, The modeling of electrostatic interactions in the function of globular proteins, *Prog. Biophys. Mol. Biol.* 48 (1986) 37–66.
- [68] M. Schaefer, M. Karplus, A comprehensive analytical treatment of continuum electrostatics, *J. Phys. Chem.* 100 (1996) 1578–1599.
- [69] T. HaDuong, S. Phan, M. Marchi, D. Borgis, Electrostatics on particles: phenomenological and orientational density functional theory approach, *J. Chem. Phys.* 117 (2002) 541–556.
- [70] A. Warshel, G. Naray-Szabo, F. Sussman, J.-K. Hwang, How do serine proteases really work? *Biochemistry* 28 (1989) 3629–3673.
- [71] P.A. Kollman, I. Massova, C. Reyes, B. Kuhn, S. Huo, L. Chong, M. Lee, T. Lee, Y. Duan, W. Wang, O. Donini, P. Cieplak, J. Srinivasan, D.A. Case, T.E. Cheatham III, Calculating structures and free energies of complex molecules: combining molecular mechanics and continuum models, *Acc. Chem. Res.* 33 (2000) 889–897.
- [72] M.K. Gilson, A. Rashin, R. Fine, B. Honig, On the calculation of electrostatic interactions in proteins, *J. Mol. Bio.* 184 (1985) 503–516.

- [73] M. Gilson, K.A. Sharp, B. Honig, Calculating the electrostatic potential of molecules in solutions, *J. Comp. Chem.* 9 (1987) 327–335.
- [74] A. Warshel, A. Papazyan, I. Muegge, Microscopic and semimicroscopic redox calculations: what can and cannot be learned from continuum models, *JBIC* 2 (1997) 143–152.
- [75] M. Gilson, B. Honig, Calculation of the total electrostatic energy of a macromolecular system. Solvation energies, binding energies and conformational analysis. *Proteins: Struct. Funct. Genet.* 4 (1988) 7–18.
- [76] K.A. Sharp, B. Honig, Calculating total electrostatic energies with the nonlinear Poisson–Boltzmann equation, *J. Phys. Chem.* 94 (1990) 7684–7692.
- [77] A. Nicholls, B. Honig, A rapid finite algorithm utilizing successive over-relaxation to solve Poisson–Boltzmann equation, *J. Comp. Chem.* 12 (1991) 435–445.
- [78] B. Honig, A. Nicholls, Classical electrostatics in biology and chemistry, *Science* 268 (1995) 1144–1149.
- [79] M. Gunner, A. Nichols, B. Honig, Electrostatic potentials in *Rhodospseudomonas viridis* reaction centers: implications for the driving force and directionality of electron transfer, *J. Phys. Chem.* 100 (1996) 4277–4291.
- [80] C.R.D. Lancaster, H. Michel, B. Honig, M.R. Gunner, Calculated coupling of electron and proton transfer in the photosynthetic reaction center of *Rhodospseudomonas viridis*, *Biophys. J.* 70 (1996) 2469–2492.
- [81] E. Alexov, M.R. Gunner, Incorporating protein conformational flexibility into the calculation of pH-dependent protein properties, *Biophys. J.* 72 (1997) 2075.
- [82] B. Rabenstein, G.M. Ullmann, E.W. Knapp, Energetics of electron-transfer and protonation reactions of the quinones in the photosynthetic reaction-center of *Rhodospseudomonas viridis*, *Biochemistry* 37 (1998) 2488–2495.
- [83] E.G. Alexov, M.R. Gunner, Calculated protein and proton motions coupled to electron transfer: electron transfer from QA- to QB in bacterial photosynthetic reaction centers, *Biochemistry* 38 (1999) 8253–8270.
- [84] J.E. Nielsen, K.V. Andersen, B. Honig, R.V. Hooft, G. Klebe, G. Vriend, R.C. Wade, Improving macromolecular electrostatics calculations, *Protein Eng.* 12 (1999) 657–662.
- [85] G.M. Ullmann, E. Knapp, Electrostatic models for computing protonation and redox equilibria in proteins, *Eur. Biophys. J. Biophys. Lett.* 28 (1999) 533–551.
- [86] M. Gunner, E.G. Alexov, A pragmatic approach to structure based calculation of coupled proton and electron transfer in proteins, *Biophys. Acta* 1485 (2000) 63–87.
- [87] R.E. Georgescu, E.G. Alexov, M.R. Gunner, Combining conformational flexibility and continuum electrostatics for calculating pK(a)s in proteins, *Biophys. J.* 83 (2002) 1731–1748.
- [88] W. Rocchia, S. Sridharan, A. Nicholls, E.G. Alexov, A. Chiabrera, B. Honig, Rapid grid-based construction of the molecular surface and the use of induced surface charge to calculate reaction field energies: applications to the molecular systems and geometric objects, *J. Comp. Chem.* 23 (2002) 128–137.
- [89] P. Voigt, E. Knapp, Tuning heme redox potentials in the cytochrome *c* subunit of photosynthetic reaction centers, *J. Biol. Chem.* 278 (2003) 51993–52001.
- [90] J. Kim, J. Mao, M. Gunner, Are acidic and basic groups in buried proteins predicted to be ionized? *J. Mol. Biol.* 348 (2005) 1283–1298.
- [91] W. Rocchia, E.G. Alexov, B. Honig, Extending the applicability of the nonlinear Poisson–Boltzmann equation: multiple dielectric constants and multivalent ions, *J. Phys. Chem., B* 105 (2001) 6507–6514.
- [92] J.D. Madura, J.M. Briggs, R.C. Wade, M.E. Davis, B.A. Luitis, J.A. McCammon, Electrostatics and diffusion of molecules in solution: simulations with the University of Houston Brownian Dynamics Program, *Comput. Phys. Commun.* 91 (1995) 57–95.
- [93] N.A. Baker, D. Sept, S. Joseph, M.J. Holst, J.A. McCammon, Electrostatics of manosystems: application to microtubules and the ribosome, *Proc. Natl. Acad. Sci. U. S. A.* 98 (2001) 10037–10041.
- [94] E.L. Mehler, G. Eichele, Electrostatic effects in water-accessible regions of proteins, *Biochemistry* 23 (1984) 3887–3891.
- [95] B.E. Hingerty, R.H. Richie, T.L. Ferrell, J.E. Turner, Dielectric effects in biopolymers. The theory of ionic saturation revisited, *Biopolymers* 24 (1985) 427–439.
- [96] E.L. Mehler, F. Guarnieri, A self-consistent, microscopic modulated screened Coulomb potential approximation to calculate pH-dependent electrostatic effects in proteins, *Biophys. J.* 75 (1999) 3–22.
- [97] J. Guenot, P. Kollman, Molecular dynamics studies of a DNA-binding protein. 2. An evaluation of implicit and explicit solvent models for the molecular-dynamics simulation of the *Escherichia coli* Trp repressor, *Protein Sci.* 1 (1992) 1185–1205.
- [98] J. Guenot, P. Collman, Conformational and energetic effects of truncating nonbonded interactions in an aqueous protein dynamics simulation, *J. Comput. Chem.* 14 (1993) 295–311.
- [99] E.T. Johnson, W.W. Parson, Electrostatic Interactions in an Integral Membrane Protein, *Biochemistry* 41 (2002) 6483–6494.
- [100] R. Constanciel, R. Contreras, Self-consistent field theory of solvent effects representation by continuum models: introduction of desolvation contribution, *Theor. Chim. Acta* 65 (1984) 1–11.
- [101] T. Kozaki, K. Morihashi, O. Kikuchi, An MNDO effective charge model study of the solvent effect. The internal rotation about partial double bonds and the nitrogen inversion in amine, *J. Mol. Struct.* 168 (1988) 265–277.
- [102] T. Kozaki, K. Morihashi, O. Kikuchi, MNDO effective charge model study of solvent effect on the potential energy surface of the SN2 reaction, *J. Am. Chem. Soc.* 111 (1989) 1547–1552.
- [103] W.C. Still, A. Tempczyk, R.C. Hawley, T. Hendrickson, Semianalytical treatment of solvation for molecular mechanics and dynamics, *J. Am. Chem. Soc.* 112 (1990) 6127–6129.
- [104] G.D. Hawkins, C.J. Cramer, D.G. Truhlar, Parametrized models of aqueous free-energies of solvation based on pairwise descreening of solute atomic charges from a dielectric medium, *J. Phys. Chem.* 100 (1996) 19824–19839.
- [105] D. Qiu, P.S. Shenkin, F.P. Hollinger, W.C. Still, The GB/SA continuum model for solvation. A fast analytical method for the calculation of approximate Born radii, *J. Phys. Chem.* 101 (1997) 3005–3014.
- [106] A. Ghosh, C.S. Rapp, R.A. Friesner, Generalized Born Model based on a surface integral formulation, *J. Phys. Chem., B* 102 (1998) 10983–10990.
- [107] D. Bashford, D.A. Case, Generalized born models of macromolecular solvation effects, *Annu. Rev. Phys. Chem.* 51 (2000) 129–152.
- [108] A. Onufriev, D.A. Case, D. Bashford, Effective Born radii in the generalized Born approximation: the importance of being perfect, *J. Comp. Chem.* 23 (2002) 1297–1304.
- [109] E. Gallicchio, R.M. Levy, AGBNP: an analytic implicit solvent model suitable for molecular dynamics simulations and high-resolution modeling, *J. Comp. Chem.* 25 (2004) 479–499.
- [110] H. Fan, A.E. Mark, J. Zhu, B. Honig, Comparative study of generalized Born models: protein dynamics, *Proc. Natl. Acad. Sci. U. S. A.* 102 (2005) 6760–6764.
- [111] J. Zhu, E.G. Alexov, B. Honig, Comparative study of generalized Born models: born radii and peptide folding, *J. Phys. Chem., B* 109 (2005) 3008–3022.
- [112] M. Born, Volumen und Hydrationswärme der Ionen, *Z. Phys.* 1 (1920) 45–47.
- [113] D. Borgis, N. Levy, M. Marchi, Computing the electrostatic free-energy of complex molecules: the variational Coulomb field approximation, *J. Chem. Phys.* 119 (2003) 3516–3528.
- [114] G. King, F.S. Lee, A. Warshel, Microscopic simulations of macroscopic dielectric constants of solvated proteins, *J. Chem. Phys.* 95 (1991) 4366–4377.
- [115] Y.Y. Sham, I. Muegge, A. Warshel, The effect of protein relaxation on charge–charge interactions and dielectric constants of proteins, *Biophys. J.* 74 (1998) 1744–1753.
- [116] I. Muegge, T. Schweins, R. Langen, A. Warshel, Electrostatic control of GTP and GDP binding in the oncoprotein p21 ras, *Structure* 4 (1996) 475–489.
- [117] T. Simonson, C.L. Brooks, Charge screening and the dielectric constant of proteins: insights from molecular dynamics, *J. Am. Chem. Soc.* 118 (1996) 8452–8458.
- [118] P.E. Smith, R.M. Brunne, A.E. Mark, Dielectric properties of trypsin

- inhibitor and lysozyme calculated from molecular dynamics simulations, *J. Phys. Chem.* 97 (1993) 2009–2014.
- [119] T. Simonson, D. Perahia, A.T. Brunger, Microscopic theory of the dielectric properties of proteins, *Biophys. J.* 59 (1991) 670–690.
- [120] T. Simonson, D. Perahia, Internal and Interfacial Dielectric Properties of cytochrome *c* from molecular dynamics simulations in aqueous solution, *Proc. Natl. Acad. Sci. U. S. A.* 92 (1995) 1082–1086.
- [121] I. Muegge, P.X. Qi, A.J. Wand, Z.T. Chu, A. Warshel, The reorganization energy of cytochrome *c* revisited, *J. Phys. Chem., B* 101 (1997) 825–836.
- [122] J. Antosiewicz, J.A. McCammon, M.K. Gilson, Prediction of pH-dependent properties of proteins, *J. Mol. Biol.* 238 (1994) 415–436.
- [123] B.E. Cohen, T.B. McAnaney, E.S. Park, Y.N. Jan, S.G. Boxer, L.Y. Jan, Probing protein electrostatics with a synthetic fluorescent amino acid, *Science* 296 (2002) 1700–1703.
- [124] S. Borman, Fluorescent probe for proteins: nonnatural amino acid used to investigate electrostatic properties within proteins, *C&EN* 80 (2002) 30.
- [125] S. Harvey, P. Hoekstra, Dielectric relaxation spectra of water adsorbed on lysozyme, *J. Phys. Chem.* 76 (1972) 2987–2994.
- [126] M. Gilson, B. Honig, The dielectric constant of a folded protein, *Biopolymers* 25 (1986) 2097–2119.
- [127] J.W. Pitera, M. Falta, W.F.v. Gunsteren, Dielectric properties of proteins from simulation: the effects of solvent, ligands, pH, and temperature, *Biophys. J.* 80 (2001) 2546–2555.
- [128] B. Garcia-Moreno, J.J. Dwyer, A.G. Gittis, E.E. Lattman, D.S. Spencer, W.E. Stites, Experimental measurement of the effective dielectric in the hydrophobic core of a protein, *Biophys. Chem.* 64 (1997) 211–224.
- [129] M. Kato, A. Warshel, Using a charging coordinate in studies of ionization induced partial unfolding, *J. Phys. Chem., B* 110 (2006) 11566–11570.
- R. Penfold, J. Warwicker, B. Jonsson, Electrostatic models for calcium binding proteins, *J. Phys. Chem., B* 108 (1998) 8599–8610.
- [131] P.J.W. Debye, L. Pauling, The inter-ionic attraction theory of ionized solutes. IV. The influence of variation of dielectric constant on the limiting law for small concentrations, *J. Am. Chem. Soc.* 47 (1925) 2129–2134.
- [132] T.J. Webb, The free energy of hydration of ions and the electrostriction of the solvent, *J. Am. Chem. Soc.* 48 (1926) 2589–2603.
- [133] T.L. Hill, The electrostatic contribution to hindered rotation in certain ions and dipolar ions in solution iii, *J. Chem. Phys.* 12 (1944) 56–61.
- [134] V.H. Teixeira, C.A. Cunha, M. Machuqueiro, A.S.F. Oliveira, B.L. Victor, C.M. Soares, A.A. Baptista, On the use of different dielectric constants for computing individual and pairwise terms in Poisson–Boltzmann studies of protein ionization equilibrium, *J. Phys. Chem., B* 109 (2005) 14691–14706.
- [135] B. Honig, K. Sharp, R. Sampogna, M.R. Gunner, A.S. Yang, On the calculation of pK<sub>a</sub>s in proteins, *Proteins: Struct. Funct. Genet.* 15 (1993) 252–265.
- [136] A. Warshel, Computer modeling of chemical reactions in enzymes and solutions, John Wiley and Sons, New York, 1991.
- [137] E.M. Kosower, Introduction to Physical Organic Chemistry, Wiley, New York, 1968.
- [138] N. Mataga, T. Kubota, Molecular Interactions and Electronic Spectra, M. Dekker, New York, 1970.
- [139] A. Pullman, B. Pullman, New paths in the molecular orbital approach to solvation in biological molecules, *Q. Rev. Biol.* 7 (1975) 506–566.
- [140] W.L. Jorgensen, Ab initio molecular orbital study of the geometric properties and protonation of alkyl chloride, *J. Am. Chem. Soc.* 100 (1978) 1057–1061.
- [141] J. Tomasi, B. Mennucci, R. Cammi, M. Cossi, Quantum mechanical models for reactions in solution, in: G. Naray-Szabo, A. Warshel (Eds.), Computational Approaches to Biochemical Reactivity, Kluwer Academic Publishers, Dordrecht, 1997.
- [142] C.J. Cramer, D.G. Truhlar, General parameterized SCF model for free energies of solvation in aqueous solution, *J. Am. Chem. Soc.* 113 (1991) 8305–8311.
- [143] B. Honig, K. Sharp, A.-S. Yang, Macroscopic models of aqueous solutions: biological and chemical applications, *J. Phys. Chem.* 97 (1993) 1101–1109.
- [144] J. Åqvist, Ion–water interaction potentials derived from free energy perturbation simulations, *J. Chem. Phys.* 94 (1990) 8021–8024.
- [145] F. Figueirido, G.S. Del Buono, R.M. Levy, On finite-size effects in computer simulations using the Ewald potential, *J. Chem. Phys.* 103 (1995) 6133–6142.
- [146] J. Åqvist, T. Hansson, On the validity of electrostatic linear response in polar solvents, *J. Phys. Chem.* 100 (1996) 9512–9521.
- [147] M. Orozco, F.J. Luque, Generalized linear-response approximation in discrete methods, *Chem. Phys. Lett.* 265 (1997) 473–480.
- [148] J. Florián, A. Warshel, Langevin dipoles model for ab initio calculations of chemical processes in solution: parametrization and application to hydration free energies of neutral and ionic solutes, and conformational analysis in aqueous solution, *J. Phys. Chem., B* 101 (1997) 5583–5595.
- [149] N.O.J. Malcolm, J.J.W. McDouall, Assessment of the Langevin dipoles solvation model for Hartree–Fock wavefunctions, *J. Mol. Struct. (Theochem)* 336 (1996) 1–9.
- [150] B. Marten, K. Kim, C. Cortis, R.A. Friesner, R.B. Murphy, M.N. Ringnalda, D. Sitkoff, B. Honig, New model for calculation of solvation free energies: correction of self-consistent reaction field continuum dielectric theory for short-range hydrogen bonding effects, *J. Phys. Chem.* 100 (1996) 11775–11788.
- [151] M. Fothergill, M.F. Goodman, J. Petruska, A. Warshel, Structure–energy analysis of the role of metal ions in phosphodiester bond hydrolysis by DNA polymerase I, *J. Am. Chem. Soc.* 117 (1995) 11619–11627.
- [152] J. Åqvist, M. Fothergill, Computer simulation of the triosephosphate isomerase catalyzed reaction, *J. Biol. Chem.* 271 (1996) 10010–10016.
- [153] C.N. Schutz, A. Warshel, The low barrier hydrogen bond (LBHB) proposal revisited: the case of the Asp, His pair in serine proteases, *Proteins* 55 (2004) 711–723.
- [154] V. Luzhkov, J. Åqvist, K<sup>+</sup>/Na<sup>+</sup> selectivity of the KcsA potassium channel from microscopic free energy perturbation calculations, *Biochim. Biophys. Acta* 1548 (2001) 194–202.
- [155] A. Burykin, C.N. Schutz, J. Villa, A. Warshel, Simulations of ion current in realistic models of ion channels: the KcsA potassium channel, *Proteins: Struct. Funct. Genet.* 47 (2002) 265–280.
- [156] V.B. Luzhkov, J. Åqvist, A computational study of ion binding and protonation states in the KcsA potassium channel, *Biochim. Biophys. Acta* 1481 (2000) 360–370.
- [157] P. Beroza, D.R. Fredkin, Calculation of amino acid pK(a)s in a protein from a continuum electrostatic model: method and sensitivity analysis, *J. Comp. Chem.* 17 (1996) 1229–1244.
- [158] A. Koumanov, H. Ruterjans, A. Karshikoff, Continuum electrostatic analysis of irregular ionization and proton allocation in proteins, *Proteins: Struct. Funct. Genet.* 46 (2002) 85–96.
- [159] T.J. You, D. Bashford, Conformation and hydrogen ion titration of proteins: a continuum electrostatic model with conformational flexibility, *Biophys. J.* 69 (1995) 1721–1733.
- [160] H.W.T. van Vlijmen, M. Schaefer, M. Karplus, Improving the accuracy of protein pK(a) calculations: conformational averaging versus the average structure, *Proteins* 33 (1998) 145–158.
- [161] H.X. Zhou, M. Vijayakumar, Modeling of protein conformational fluctuations in pK(a) predictions, *J. Mol. Biol.* 267 (1997) 1002–1011.
- [162] J.J. Wendoloski, J.B. Matthew, Molecular-dynamics effects on protein electrostatics, *Proteins* 5 (1989) 313–321.
- [163] J.J. Dwyer, A.G. Gittis, D.A. Karp, E.E. Lattman, D.S. Spencer, W.E. Stites, E.B. Garcia-Moreno, High apparent dielectric constants in the interior of a protein reflect water penetration [In Process Citation], *Biophys. J.* 79 (2000) 1610–1620.
- [164] C.A. Fitch, D.A. Karp, K.K. Lee, W.E. Stites, E.E. Lattman, B. Garcia-Moreno, Experimental pK(a) values of buried residues: analysis with continuum methods and role of water penetration, *Biophys. J.* 82 (2002) 3289–3304.
- [165] S.W. Englander, M.M.G. Krishna, Hydrogen exchange, *Nature Struct. Biol.* 8 (2001) 1.
- [166] R.J. Kassner, Effects of non polar environments on the redox potentials of heme complexes, *Proc. Natl. Acad. Sci.* 69 (1972) 2263.

- [167] R.J. Kassner, A theoretical model for the effects of local nonpolar heme environments on the redox potentials in cytochromes, *J. Am. Chem. Soc.* 95 (1973) 2674.
- [168] H.-X. Zhou, Control of reduction potential by protein matrix: lesson from a spherical protein model, *J. Biol. Inorg. Chem.* 2 (1997) 109–113.
- [169] I. Bertini, G. Gori-Savellini, C. Luchinat, Are unit charges always negligible? *J. Biol. Inorg. Chem.* 2 (1997) 114–118.
- [170] A.G. Mauk, G.R. Moore, Control of metalloprotein redox potentials: what does site-directed mutagenesis of hemoproteins tell us? *J. Biol. Inorg. Chem.* 2 (1997) 119–125.
- [171] M.R. Gunner, E. Alexov, E. Torres, S. Lipovaca, The importance of the protein in controlling the electrochemistry of heme metalloproteins: methods of calculation and analysis, *J. Biol. Inorg. Chem.* 2 (1997) 126–134.
- [172] G. Naray-Szabo, Electrostatic modulation of electron transfer in the active site of heme peroxidases, *J. Biol. Inorg. Chem.* 2 (1997) 135–138.
- [173] F.A. Armstrong, Evaluations of reduction potential data in relation to coupling, kinetics and function, *J. Biol. Inorg. Chem.* 2 (1997) 139–142.
- [174] N.K. Rogers, G.R. Moore, On the energetics of conformational-changes and Ph dependent redox behavior of electron-transfer proteins, *FEBS Lett.* 228 (1988) 69–73.
- [175] A.K. Churg, R.M. Weiss, A. Warshel, T. Takano, On the action of cytochrome *c*: correlating geometry changes upon oxidation with activation energies of electron transfer, *J. Phys. Chem.* 87 (1983) 1683–1694.
- [176] A.K. Churg, A. Warshel, Control of redox potential of cytochrome *c* and microscopic dielectric effects in proteins, *Biochemistry* 25 (1986) 1675–1681.
- [177] P.J. Stephens, D.R. Jollie, A. Warshel, Protein control of redox potentials of iron–sulfur proteins, *Chem. Rev.* 96 (1996) 2491–2513.
- [178] P.D. Swartz, B.W. Beck, T. Ichiye, Structural origins of redox potentials in Fe–S proteins—Electrostatic potentials of crystal structures, *Biophys. J.* 71 (1996) 2958–2969.
- [179] R.B. Yelle, T. Ichiye, Solvation free-energy reaction curves for electron-transfer in aqueous solution—Theory and simulation, *J. Phys. Chem., B* 101 (1997) 4127–4135.
- [180] W.W. Parson, Z.T. Chu, A. Warshel, Reorganization energy of the initial electron-transfer step in photosynthetic bacterial reaction centers, *Biophys. J.* 74 (1998) 182–191.
- [181] A. Warshel, W.W. Parson, Dynamics of biochemical and biophysical reactions: insight from computer simulations, *Q. Rev. Biophys.* 34 (2001) 563–670.
- [182] L. Noodleman, T. Lovell, T.Q. Liu, F. Himo, R.A. Torres, Insights into properties and energetics of iron–sulfur proteins from simple clusters to nitrogenase, *Curr. Opin. Chem. Biol.* 6 (2002) 259–273.
- [183] V.H. Teixeira, C.M. Soares, A.M. Baptista, Studies of the reduction and protonation behavior of tetraheme cytochromes using atomic detail, *J. Biol. Inorg. Chem.* 7 (2002) 200–216.
- [184] S. Creighton, J.-K. Hwang, A. Warshel, W.W. Parson, J. Norris, Simulating the dynamics of the primary charge separation process in bacterial photosynthesis, *Biochemistry* 27 (1988) 774–781.
- [185] W.W. Parson, Z.T. Chu, A. Warshel, Electrostatic control of charge separation in bacterial photosynthesis, *Biochim. Biophys. Acta* 1017 (1990) 251–272.
- [186] M. Marchi, J.N. Gehlen, D. Chandler, M. Newton, Diabatic surfaces and the pathway for primary electron transfer in a photosynthetic reaction center, *J. Am. Chem. Soc.* 115 (1993) 4178–4190.
- [187] H. Treutlein, K. Schulten, J. Deisenhofer, H. Michel, A. Brünger, M. Karplus, Molecular dynamics simulation of the primary processes in the photosynthetic reaction center of *Rhodospseudomonas viridis*, in: J. Breton, A. Verméglio (Eds.), *The Photosynthetic Reaction Center. Structure and Dynamics*, Plenum Press, London, 1988, pp. 139–150.
- [188] H. Treutlein, K. Schulten, C. Niedermeier, J. Deisenhofer, H. Michel, D. DeVault, Electrostatic control of electron transfer in the photosynthetic reaction center of *Rhodospseudomonas viridis*, in: J. Breton, A. Verméglio (Eds.), *The Photosynthetic Bacterial Reaction Center*, Plenum Press, London, 1988, pp. 369–377.
- [189] R.A. Alden, W.W. Parson, Z.T. Chu, A. Warshel, Macroscopic and microscopic estimates of the energetics of charge separation in bacterial reaction centers, in: M.E. Michel-Beyerle (Ed.), *The Reaction Center of Photosynthetic Bacteria: Structure and Dynamics*, Springer, Berlin, 1995, pp. 105–116.
- [190] M. Tachiya, Relation between the electron transfer rate and the free energy change of reaction, *J. Phys. Chem.* 93 (1989) 7050–7052.
- [191] H.X. Zhou, A. Szabo, Microscopic formulation of Marcus theory of electron-transfer, *J. Chem. Phys.* 103 (1995) 3481–3494.
- [192] M. Ceccarelli, M. Marchi, Simulation and modeling of the *Rhodobacter sphaeroides* bacterial reaction center II: Primary charge separation, *J. Phys. Chem., B* 107 (2003) 5630–5641.
- [193] R.G. Alden, W.W. Parson, Z.T. Chu, A. Warshel, Macroscopic and microscopic estimates of the energetics of charge separation in bacterial reaction centers, in: M.E. Beyerle (Ed.), *Reaction Centers of Photosynthetic Bacteria Structure and Dynamics*, Springer Verlag, Berlin, 1996.
- [194] J.I. Chuang, S.G. Boxer, D. Holtzen, C. Kirmaier, High yield of M-side electron transfer in mutants of *Rhodobacter capsulatus* reaction centers lacking the L-side bacteriopheophytin, *Biochemistry* 45 (2006) 3845–3851.
- [195] M.H.M. Olsson, G. Hong, A. Warshel, Frozen density functional free energy simulations of redox proteins: computational studies of the reduction potential of plastocyanin and rusticyanin, *J. Am. Chem. Soc.* 125 (2003) 5025–5039.
- [196] I. Muegge, M. Rarey, Small Molecule Docking and Scoring, in (K.B. Lipkowitz, D.B. Boyd, eds.), *Reviews in computational chemistry*, Wiley-VCH, John Wiley and Sons, New York, 2001, pp.1–60.
- [197] Y.Y. Sham, Z.T. Chu, H. Tao, A. Warshel, Examining methods for calculations of binding free energies: LRA, LIE, PDL-LRA, and PDL/S-LRA calculations of ligands binding to an HIV protease, *Proteins: Struct. Funct. Genet.* 39 (2000) 393–407.
- [198] J. Åqvist, C. Medina, J.-E. Samuelsson, A new method for predicting binding affinity in computer-aided drug design, *Prot. Eng.* 7 (1994) 385–391.
- [199] B.O. Brandsdal, F. Osterberg, M. Almlof, I. Feierberg, V.B. Luzhkov, J. Åqvist, Free energy calculations and ligand binding, *Protein Simulations* (2003) 123–158.
- [200] M. Almlof, J. Åqvist, A.O. Smalas, B.O. Brandsdal, Probing the effect of point mutations at protein–protein interfaces with free energy calculations, *Biophys. J.* 90 (2006) 433–442.
- [201] J.D. Madura, Y. Nakajima, R.M. Hamilton, A. Wierzbicki, A. Warshel, Calculations of the electrostatic free energy contributions to the binding free energy of sulfonamides to carbonic anhydrase, *Struc. Chem.* 7 (1996) 131–137.
- [202] J. Florian, M.F. Goodman, A. Warshel, Theoretical Investigation of the binding free energies and key substrate-recognition components of the replication fidelity of human DNA polymerase  $\beta$ , *J. Phys. Chem., B* 106 (2002) 5739–5753.
- [203] J. Florian, A. Warshel, M.F. Goodman, Molecular dynamics free-energy simulations of the binding contribution to the fidelity of T7 DNA polymerase, *J. Phys. Chem., B* 106 (2002) 5754–5760.
- [204] J. Florian, M.F. Goodman, A. Warshel, Computer simulation studies of the fidelity of DNA polymerases, *Biopolymers* 68 (2003) 286–299.
- [205] A. Warshel, P.K. Sharma, M. Kato, Y. Xiang, H. Liu, M.H.M. Olsson, Electrostatic Basis for enzyme catalysis, *Chem. Rev.* 106 (2006) 3210–3235.
- [206] M. Kato, S. Braun-Sand, A. Warshel, Challenges and Progresses in Calculations of Binding Free Energies; What Does it Take to Quantify Electrostatic Contributions to Protein Ligand Interactions, in: *Computation Biology: Structure-based Drug Design*, Royal Society of Chemistry, England, 2006, in press.
- [207] J. Hermans, L. Wang, Inclusion of loss of translational and rotational freedom in theoretical estimates of free energies of binding. Application to a complex of benzene and mutant T4 lysozyme, *J. Am. Chem. Soc.* 119 (1997) 2707–2714.
- [208] M. Štrajbl, Y.Y. Sham, J. Villà, Z.T. Chu, A. Warshel, Calculations of activation entropies of chemical reactions in solution, *J. Phys. Chem., B* 104 (2000) 4578–4584.

- [209] J. Carlsson, J. Aqvist, Absolute and relative entropies from computer simulation with applications to ligand binding, *J. Phys. Chem., B* 109 (2005) 6448–6456.
- [210] M.K. Gilson, J.A. Given, B.L. Bush, J.A. McCammon, The statistical-thermodynamic basis for computation of binding affinities: a critical review, *Biophys. J.* 72 (1997) 1047–1069.
- [211] H.B. Luo, K. Sharp, On the calculation of absolute macromolecular binding free energies, *Proc. Natl. Acad. Sci. U. S. A.* 99 (2002) 10399–10404.
- [212] S.H. Fleischman, C.L. Brooks, Thermodynamics of aqueous solvation—Solution properties of alcohols and alkanes, *J. Chem. Phys.* 87 (1987) 3029–3037.
- [213] R.M. Levy, E. Gallicchio, Computer simulations with explicit solvent: Recent progress in the thermodynamic decomposition of free energies and in modeling electrostatic effects, *Annu. Rev. Phys. Chem.* 49 (1998) 531–567.
- [214] R.M. Levy, M. Karplus, J. Kushick, D. Perahia, Evaluation of the configurational entropy for proteins—Application to molecular-dynamics simulations of an alpha-helix, *Macromolecules* 17 (1984) 1370–1374.
- [215] M. Karplus, J.N. Kushick, Method for estimating the configurational entropy of macromolecules, *Macromolecules* 14 (1981) 325–332.
- [216] J. Schlitter, Estimation of absolute and relative entropies of macromolecules using the covariance-matrix, *Chem. Phys. Lett.* 215 (1993) 617–621.
- [217] D. Bakowies, W.F. van Gunsteren, Simulations of apo and holo-fatty acid binding protein: structure and dynamics of protein, ligand and internal water, *J. Mol. Biol.* 315 (2002) 713–736.
- [218] H. Schafer, X. Daura, A.E. Mark, W.F. van Gunsteren, Entropy calculations on a reversibly folding peptide: changes in solute free energy cannot explain folding behavior, *Proteins: Struct. Funct. Genet.* 43 (2001) 45–56.
- [219] H. Schafer, A.E. Mark, W.F. van Gunsteren, Absolute entropies from molecular dynamics simulation trajectories, *J. Chem. Phys.* 113 (2000) 7809–7817.
- [220] A. Warshel, Office of Naval Research, Award Number N00014-91-J-1318, , 1991.
- [221] J. Villa, M. Strajbl, T.M. Glennon, Y.Y. Sham, Z.T. Chu, A. Warshel, How important are entropic contributions to enzyme catalysis? *Proc. Natl. Acad. Sci. U. S. A.* 97 (2000) 11899–11904.
- [222] P.K. Sharma, Y. Xiang, M. Kato, A. Warshel, What are the roles of substrate-assisted catalysis and proximity effects in peptide bond formation by the Ribosome? *Biochemistry* 44 (2005) 11307–11314.
- [223] A. Warshel, Computer simulations of enzyme catalysis: methods, progress, and insights, *Annu. Rev. Biophys. Biomol. Struct.* 32 (2003) 425–443.
- [224] A. Fersht, *Structure and Mechanism in Protein Science. A Guide to Enzyme Catalysis and Protein Folding*, W.H. Freeman and Company, New York, 1999.
- [225] M. Field, Stimulating enzyme reactions: challenges and perspectives, *J. Comp. Chem.* 23 (2002) 48–58.
- [226] P.A. Bash, M.J. Field, R.C. Davenport, G.A. Petsko, D. Ringe, M. Karplus, Computer simulation and analysis of the reaction pathway of triosephosphate isomerase, *Biochemistry* 30 (1991) 5826–5832.
- [227] D.S. Hartsough, K.M. Merz Jr., Dynamic force field models: molecular dynamics simulations of human carbonic anhydrase II using a quantum mechanical/molecular mechanical coupled potential, *J. Phys. Chem.* 99 (1995) 11266–11275.
- [228] C. Alhambra, J. Gao, J.C. Corchado, J. Villà, D.G. Truhlar, Quantum mechanical dynamical effects in an enzyme-catalyzed proton transfer reaction, *J. Am. Chem. Soc.* 121 (1999) 2253–2258.
- [229] S.A. Marti, J. Moliner, V. Silla, E. Tunon, I. Bertran, J., Transition structure selectivity in enzyme catalysis: a QM/MM study of chorismate mutase, *Theor. Chem. Acc.* 3 (2001) 207–212.
- [230] A.J. Mulholland, G.H. Grant, W.G. Richards, Computer modelling of enzyme catalysed reaction mechanisms, *Prot. Eng.* 6 (1993) 133–147.
- [231] U.C. Singh, P.A. Kollman, A combined *Ab Initio* quantum mechanical and molecular mechanical method for carrying out simulations on complex molecular systems: applications to the  $\text{CH}_3\text{Cl}+\text{Cl}^-$  exchange reaction and gas phase protonation of polyethers, *J. Comput. Chem.* 7 (1986) 718–730.
- [232] A. Warshel, Energetics of enzyme catalysis, *Proc. Natl. Acad. Sci. U. S. A.* 75 (1978) 5250–5254.
- [233] A. Warshel, Electrostatic origin of the catalytic power of enzymes and the role of preorganized active sites, *J. Biol. Chem.* 273 (1998) 27035–27038.
- [234] M. Roca, S. Marti, J. Andres, V. Moliner, M. Tunon, J. Bertran, A.H. Williams, Theoretical modeling of enzyme catalytic power: analysis of “cratic” and electrostatic factors in catechol O-methyltransferase, *J. Am. Chem. Soc.* 125 (2003) 7726–7737.
- [235] W. Cannon, S. Benkovic, Solvation, reorganization energy, and biological catalysis, *J. Biol. Chem.* 273 (1998) 26257–26260.
- [236] G. Nàray-Szabó, M. Fuxreiter, A. Warshel, Electrostatic basis of enzyme catalysis, in: G. Nàray-Szabó, A. Warshel (Eds.), *Computational Approaches to Biochemical Reactivity*, Kluwer Academic Publishers, Dordrecht, 1997, pp. 237–293.
- [237] J. Van Beek, R. Callender, M.R. Gunner, The contribution of electrostatic and van der Waals interactions to the stereospecificity of the reaction catalyzed by lactate-dehydrogenase, *Biophys. J.* 72 (1997) 619–626.
- [238] C.L. Fisher, D.E. Cabelli, R.A. Hallewell, P. Beroza, E.D. Getzoff, J.A. Tainer, Computational, pulse-radiolytic, and structural investigations of lysine-136 and its role in the electrostatic triad of human Cu, Zn superoxide dismutase, *Proteins: Struct. Funct. Genet.* 29 (1997) 103–112.
- [239] J. Antosiewicz, J.A. McCammon, S.T. Wlodek, M.K. Gilson, Simulation of charge-mutant acetylcholinesterases, *Biochemistry* 34 (1995) 4211–4219.
- [240] M. Fuxreiter, A. Warshel, Origin of the catalytic power of acetylcholinesterase: computer simulation studies, *J. Am. Chem. Soc.* 120 (1998) 183–194.
- [241] A. Warshel, J. Villà, M. Štrajbl, J. Florián, Remarkable rate enhancement of orotidine 5'-monophosphate decarboxylase is due to transition state stabilization rather than ground state destabilization, *Biochemistry* 39 (2000) 14728–14738.
- [242] Q. Cui, M. Elstner, E. Kaxiras, T. Frauenheim, M. Karplus, A QM/MM implementation of the self-consistent charge density functional tight binding (SCC-DFTB) method, *J. Phys. Chem., B* 105 (2001) 569–585.
- [243] S. Hammes-Schiffer, Quantum-classical simulation methods for hydrogen transfer in enzymes: a case study of dihydrofolate reductase, *Curr. Opin. Struct. Biol.* 14 (2004) 192–201.
- [244] K.F. Wong, T. Selzer, S.J. Benkovic, S. Hammes-Schiffer, Impact of distal mutations on the network of coupled motions correlated to hydride transfer in dihydrofolate reductase, *Proc Natl. Acad. Sci. U. S. A.* 102 (2005) 6807–6812.
- [245] I.F. Thorpe, C.L. Brooks, Conformational substates modulate hydride transfer in dihydrofolate reductase, *J. Am. Chem. Soc.* 127 (2005) 12997–13006.
- [246] A. Warshel, R.M. Weiss, Energetics of heme-protein interactions in hemoglobin, *J. Am. Chem. Soc.* 103 (1981) 446.
- [247] T.M. Glennon, J. Villa, A. Warshel, How does GAP catalyze the GTPase reaction of Ras? A computer simulation study, *Biochemistry* 39 (2000) 9641–9651.
- [248] M. Strajbl, A. Shurki, A. Warshel, Converting conformational changes to electrostatic energy in molecular motors: the energetics of ATP synthase, *Proc. Natl. Acad. Sci. U. S. A.* 100 (2003) 14834–14839.
- [249] A. Shurki, A. Warshel, Why does the Ras switch “break” by oncogenic mutations? *Proteins: Struct. Funct. Bioinf.* 55 (2004) 1–10.
- [250] Y. Xiang, P. Oelschlaeger, J. Florian, M.F. Goodman, A. Warshel, Simulating the effect of DNA polymerase mutations on transition state energetics and fidelity: evaluating amino acid group contribution and allosteric coupling for ionized residues in human Pol  $\beta$ , *Biochemistry* 45 (2006) 7036–7048.
- [251] I.T. Suydam, C.D. Snow, V.S. Pande, S.G. Boxer, Electric fields at the active site of an enzyme: direct comparison of experiment with theory, *Science* 313 (2006) 200–204.
- [252] P. Várnai, A. Warshel, Computer simulation studies of the catalytic

- mechanism of human aldose reductase, *J. Am. Chem. Soc.* 122 (2000) 3849–3860.
- [253] D.A. Kraut, P.A. Sigala, B. Pybus, C.W. Liu, D. Ringe, G.A. Petsko, D. Herschlag, Testing electrostatic complementarity in enzyme catalysis: hydrogen bonding in the ketosteroid isomerase oxyanion hole, *PLoS Biol.* 4 (2006) 0501–0519.
- [254] I. Feierberg, J. Åqvist, The catalytic power of ketosteroid isomerase investigated by computer simulation, *Biochemistry* 41 (2002) 15728–15735.
- [255] M.F. Perutz, J.V. Kilmartin, K. Nishikura, J.H. Fogg, P.J.G. Butler, H.S. Rollema, Identification of residues contributing to the Bohr effect of human-hemoglobin, *J. Mol. Biol.* 138 (1980) 649–670.
- [256] A. Warshel, N. Barboy, Energy storage and reaction pathways in the first step of the vision process, *J. Am. Chem. Soc.* 104 (1982) 1469.
- [257] A. Warshel, Charge stabilization mechanism in the visual and purple membrane pigments, *Proc. Natl. Acad. Sci. U. S. A.* 75 (1978) 2558.
- [258] A. Warshel, Calculations of enzymic reactions: calculations of  $pK_a$ , proton transfer reactions, and general acid catalysis reactions in enzymes, *Biochemistry* 20 (1981) 3167–3177.
- [259] F. Jordan, H. Li, A. Brown, Remarkable stabilization of zwitterionic intermediates may account for a billion-fold rate acceleration by thiamin diphosphate-dependent decarboxylases, *Biochemistry* 38 (1999) 6369–6373.
- [260] M.J.S. Dewar, D.M. Storch, Alternative view of enzyme reactions, *Proc. Natl. Acad. Sci. U. S. A.* 82 (1985) 2225–2229.
- [261] J. Crosby, R. Stone, G.E. Lienhard, Mechanisms of thiamine-catalyzed reactions. decarboxylation of 2-(1-Carboxy-1-hydroxyethyl)-3,4-dimethylthiazolium chloride, *J. Am. Chem. Soc.* 92 (1970) 2891–2900.
- [262] J.K. Lee, K.N. Houk, A proficient enzyme revisited: the predicted mechanism for orotidine monophosphate decarboxylase, *Science* 276 (1997) 942–945.
- [263] J.-K. Hwang, A. Warshel, Why ion pair reversal by protein engineering is unlikely to succeed, *Nature* 334 (1988) 270.
- [264] R.L. Cutler, A.M. Davies, S. Creighton, A. Warshel, G.R. Moore, M. Smith, A.G. Mauk, Role of arginine-38 in regulation of the cytochrome *c* oxidation–reduction equilibrium, *Biochemistry* 28 (1989) 3188–3197.
- [265] X. Barril, C. Aleman, M. Orozco, F.J. Luque, Salt bridge interactions: stability of the ionic and neutral complexes in the gas phase, in solution, and in proteins, *Proteins* 32 (1998) 67–79.
- [266] A. Warshel and G. Naray-Szabo. Kluwer Academic Publishers 1997.
- [267] Z.S. Hendsch, B. Tidor, Do salt bridges stabilize proteins—A continuum electrostatic analysis, *Protein Sci.* 3 (1994) 211–226.
- [268] S. Kumar, R. Nussinov, Relationship between ion pair geometries and electrostatic strengths in proteins, *Biophys. J.* 83 (2002) 1595–1612.
- [269] N. Nassar, G. Horn, C. Herrmann, A. Scherer, F. McCormick, A. Wittinghofer, The 2.2 Å crystal structure of the ras-binding domain of the serine/threonine kinase c-Raf1 in complex with Rap1A and a GTP analogue, *Nature* 375 (1995) 554–560.
- [270] R.I. Menz, J.E. Walker, A.G.W. Leslie, Structure of bovine mitochondrial F1-ATPase with nucleotide bound to all three catalytic sites: implications for the mechanism of rotary catalysis, *Cell* 106 (2001) 331–341.
- [271] D. Flock, V. Helms, Protein–protein docking of electron transfer complexes: cytochrome *c* oxidase and cytochrome *c*, *Proteins: Struct. Funct. Genet.* 47 (2002) 75–85.
- [272] B.L. Victor, J.B. Vicente, R. Rodrigues, S. Oliveira, C. Rodrigues-Pousada, C. Frazao, C.M. Gomes, M. Teixeira, C.M. Soares, Docking and electron transfer studies between rubredoxin and rubredoxin: oxygen oxidoreductase, *J. Biol. Inorg. Chem.* 8 (2003) 475–488.
- [273] Z. Hu, B. Ma, H. Wolfson, R. Nussinov, Conservation of polar residues as hot spots at protein interfaces, *Proteins* 39 (2000) 331–342.
- [274] R. Guerois, J.E. Nielsen, L. Serrano, Predicting changes in the stability of proteins and their protein complexes: a study of more than 1000 mutations, *J. Mol. Biol.* 320 (2002) 369–387.
- [275] T. Kortemme, D. Baker, A simple physical model for binding energy hot spots in protein–protein complexes, *Proc. Natl. Acad. Sci. U. S. A.* 99 (2002) 14116–14121.
- [276] T. Wang, S. Tomic, R.R. Gabdoulina, R.C. Wade, How optimal are the binding energetics of barnase and barstar, *Biophys. J.* 87 (2004) 1618–1630.
- [277] F. Dong, H.-Y. Zhou, Electrostatic contributions to exposed charges versus semi-buried salt bridges, *Biophys. J.* 83 (2002) 1341–1347.
- [278] C. Wang, O. Schueler-Furman, D. Baker, Improved side-chain modeling for protein–protein docking, *Protein Sci.* 14 (2005) 1328–1339.
- [279] L.P. Ehrlich, M. Nilges, R.C. Wade, The impact of protein flexibility on protein–protein docking, *Proteins* 58 (2005) 126–133.
- [280] M. Levitt, A. Warshel, Computer simulations of protein folding, *Nature* 253 (1975) 694.
- [281] N. Go, Theoretical-studies of protein folding, *Annu. Rev. Biophys. Biol.* 12 (1983) 183–210.
- [282] J.N. Onuchic, P.G. Wolynes, Z. Luthey-Schulten, N.D. Socci, Toward an outline of the topography of a realistic protein-folding funnel, *Proc. Natl. Acad. Sci. U. S. A.* 92 (1995) 3626–3630.
- [283] A. Godzik, J. Skolnick, A. Kolinski, Simulations of the folding pathway of triose phosphate isomerase-type-alpha/beta barrel proteins, *Proc. Natl. Acad. Sci. U. S. A.* 89 (1992) 2629–2633.
- [284] J. Karanicolas, C.L. Brooks, The structural basis for biphasic kinetics in the folding of the WW domain from a formin-binding protein: lessons for protein design? *Proc. Natl. Acad. Sci. U. S. A.* 100 (2003) 3954–3959.
- [285] K.A. Dill, Dominant forces in protein folding, *Biochemistry* 29 (1990) 7133–7155.
- [286] C. Simmerling, B. Strockbine, A.E. Roitberg, All-atom structure prediction and folding simulations of a stable protein, *J. Am. Chem. Soc.* 124 (2002) 11258–11259.
- [287] C.D. Snow, N. Nguyen, V.S. Pande, M. Gruebele, Absolute comparison of simulated and experimental protein-folding dynamics, *Nature* 420 (2002) 102–106.
- [288] Z.Z. Fan, J.K. Hwang, A. Warshel, Using simplified protein representation as a reference potential for all-atom calculations of folding free energies, *Theor. Chem. Acc.* 103 (1999) 77–80.
- [289] L.J. Smith, R.M. Jones, W.F. van Gunsteren, Characterization of the denaturation of human alpha-lactalbumin in urea by molecular dynamics simulations, *Proteins: Struct. Funct. Bioinf.* 58 (2005) 439–449.
- [290] B. Zagrovic, W.F. van Gunsteren, Comparing atomistic simulation data with the NMR experiment: how much can NOEs actually tell us? *Proteins: Struct. Funct. Bioinf.* 63 (2006) 210–218.
- [291] A. Liwo, M. Khalili, H.A. Scheraga, Ab initio simulations of protein-folding pathways by molecular dynamics with the united-residue model of polypeptide chains, *Proc. Natl. Acad. Sci. U. S. A.* 102 (2005) 2265–2266.
- [292] M. Khalili, A. Liwo, H.A. Scheraga, Kinetic studies of folding of the B-domain of staphylococcal protein A with molecular dynamics and a united-residue (UNRES) model of polypeptide chains, *J. Mol. Biol.* 355 (2006) 536–547.
- [293] O. Schueler-Furman, C. Wang, P. Bradley, K. Misura, D. Baker, Progress in modeling of protein structures and interactions, *Science* 310 (2005) 638–642.
- [294] M. Shirts, V.S. Pande, Computing - Screen savers of the world unite! *Science* 290 (2000) 1903–1904.
- [295] J. Hollien, S. Marqusee, Structural distribution of stability in a thermophilic enzyme, *Proc. Nat. Acad. Sci. U. S. A.* 96 (1999) 13674–13678.
- [296] K.C. Usher, A.F.A. De la Cruz, F.W. Dahlquist, R.V. Swanson, M.I. Simon, S.J. Remington, Crystal structures of CheY from *Thermotoga maritima* do not support conventional explanations for the structural basis of enhanced thermostability, *Protein Sci.* 7 (1998) 403–412.
- [297] B. Honig, A.S. Yang, Free-energy balance in protein-folding, *Adv. Protein Chem.* 46 (1995) 27–58.
- [298] L. Xiao, B. Honig, Electrostatic contributions to the stability of hyperthermophilic proteins, *J. Mol. Biol.* 289 (1999) 1435–1444.
- [299] B. Ibarra-Molero, J.M. Sanchez-Ruiz, Genetic algorithm to design stabilizing surface-charge distributions in proteins, *J. Phys. Chem., B* 106 (2002) 6609–6613.
- [300] A. Gilletto, C.N. Pace, Buried, charged, non-ion-paired aspartic acid 76 contributes favorably to the conformational stability of ribonuclease T-1, *Biochemistry* 38 (1999) 13379–13384.

- [301] G.R. Grimsley, K.L. Shaw, L.R. Fee, R.W. Alston, B.M.P. Huyghues-Despointes, R.L. Thurlkill, J.M. Scholtz, C.N. Pace, Increasing protein stability by altering long-range coulombic interactions, *Protein Sci.* 8 (1999) 1843–1849.
- [302] A. Warshel, Conversion of light energy to electrostatic energy in the proton pump of *Halobacterium halobium*, *Photochem. Photobiol.* 30 (1979) 285–290.
- [303] G. Willmsky, H. Bang, G. Fischer, M.A. Marahiel, Characterization of Cspb, a bacillus-subtilis inducible cold shock gene affecting cell viability at low-temperatures, *J. Bacteriol.* 174 (1992) 6326–6335.
- [304] B.N. Dominy, H. Minoux, C.L. Brooks, An electrostatic basis for the stability of thermophilic proteins, *Proteins: Struct. Funct. Genet.* 57 (2004) 128–141.
- [305] B. Hille, *Ion Channels of Excitable Membranes*, 3rd ed. Sinauer Assoc., Sunderland, MA, 2001.
- [306] G. Eisenman, R. Horn, Ionic selectivity revisited: the role of kinetic and equilibrium processes in ion permeation through channels, *J. Membr. Biol.* 50 (1983) 1025–1034.
- [307] G. Eisenman, O. Alvarez, Structure and function of channels and channelogs as studied by computational chemistry, *J. Membr. Biol.* 119 (1991) 109–132.
- [308] V.B. Luzhkov, J. Åqvist, Ions and blockers in potassium channels: insights from free energy simulations, *Biochim. Biophys. Acta* 1747 (2005) 109–120.
- [309] P.C. Jordan, Microscopic approaches to ion transport through transmembrane channels. The model system gramicidin, *J. Phys. Chem.* 91 (1987) 6582–6591.
- [310] J.H. Morals-Cabral, Y. Zhou, R. MacKinnon, Energetic optimization of ion conduction rate by the K<sup>+</sup> selectivity filter, *Nature* 414 (2001) 37–42.
- [311] I.H. Shrivastava, M.S.P. Sansom, Simulations of ion permeation through a potassium channel: molecular dynamics of KcsA in a phospholipid bilayer, *Biophys. J.* 78 (2000) 557–570.
- [312] T.W. Allen, S. Kuyucak, S.H. Chung, Molecular dynamics study of the KcsA potassium channel, *Biophys. J.* 77 (1999) 2502–2516.
- [313] J. Åqvist, V. Luzhkov, Ion permeation mechanism of the potassium channel, *Nature* 404 (2000) 881–884.
- [314] A. Burykin, M. Kato, A. Warshel, Exploring the origin of the ion selectivity of the KcsA potassium channel, *Proteins* 52 (2003) 412–426.
- [315] G.D. Cymes, Y. Ni, C. Grosman, Probing ion-channel pores one proton at a time, *Nature* 438 (2005) 975–980.
- [316] P. Agre, D. Kozono, Aquaporin water channels: molecular mechanisms for human diseases, *FEBS Lett.* 555 (2003) 72–78.
- [317] K. Murata, K. Mitsuoka, T. Hirai, T. Walz, P. Agre, J.B. Heymann, A. Engel, Y. Fujiyoshi, Structural determinants of water permeation through aquaporin-1, *Nature* 407 (2000) 599–605.
- [318] H. Sui, B.-G. Han, J.K. Lee, P. Walian, B.K. Jap, Structural basis of water-specific transport through the AQP1 water channel, *Nature* 414 (2001) 872–878.
- [319] A. Yarnell, Blockade in the cell's waterway, *Chem. Eng. News* 82 (2004) 42–44.
- [320] B. de Groot, H. Grubmuller, Water permeation across biological membranes: mechanism and dynamics of aquaporin-1 and GlpF, *Science* 294 (2001) 2353–2357.
- [321] B.L. de Groot, T. Frigato, V. Helms, H. Grubmuller, The mechanism of proton exclusion in the aquaporin-1 water channel, *J. Mol. Biol.* 333 (2003) 279–293.
- [322] T.E. Decoursey, Voltage-gated proton channels and other proton transfer pathways, *Physiol. Rev.* 83 (2003) 475–579.
- [323] M.O. Jensen, E. Tajkhorshid, K. Schulten, Electrostatic tuning of permeation and selectivity in aquaporin water channels, *Biophys. J.* 85 (2003) 2884–2899.
- [324] E. Tajkhorshid, P. Nollert, M. Jensen, L. Miercke, R.M. Stroud, K. Schulten, Control of the selectivity of the aquaporin water channel by global orientational tuning, *Science* 296 (2002) 525–530.
- [325] B.L. de Groot, H. Grubmuller, The dynamics and energetics of water permeation and proton exclusion in aquaporins, *Curr. Opin. Struct. Biol.* 15 (2005) 176–183.
- [326] N. Chakrabarti, B. Roux, R. Pomes, Structural determinants of proton blockage in aquaporins, *J. Mol. Biol.* 343 (2004) 493–510.
- [327] A. Burykin, A. Warshel, On the origin of the electrostatic barrier for proton transport in aquaporin, *FEBS Lett.* 570 (2004) 41–46.
- [328] A. Burykin, A. Warshel, What really prevents proton transport through aquaporin? Charge self-energy versus proton wire proposals, *Biophys. J.* 85 (2003) 3696–3706.
- [329] G.V. Miloshevsky, P.C. Jordan, Water and ion permeation in bAQP1 and GlpF channels: a kinetic Monte Carlo study, *Biophys. J.* 87 (2004) 3690–3702.
- [330] N. Agmon, The Grothuss mechanism, *Chem. Phys. Lett.* 244 (1995) 456–462.
- [331] M. Eigen, *Angew. Chem., Int. Ed. Engl.* 3 (1964).
- [332] G. Zundel, J. Fritsch, *The Chemical Physics of Solvation*, vol. 2, Elsevier, Amsterdam, 1986.
- [333] B. Ilan, E. Tajkhorshid, K. Schulten, G.A. Voth, The mechanism of proton exclusion in aquaporin channels, *Proteins: Struct. Funct. Genet.* 55 (2004) 223–228.
- [334] Y. Sham, I. Muegge, A. Warshel, Simulating proton translocations in proteins: probing proton transfer pathways in the Rhodobacter Sphaeroides Reaction Center, *Proteins* 36 (1999) 484–500.
- [335] M. Kato, A. Pislakov, A. Warshel, The barrier for proton transport in aquaporins as a test case for electrostatic models: on the role of protein relaxation in mutational calculations, *Protein: Struct. Funct. Genet. Bioinf.* 64 (2006) 829–844.
- [336] A. Wada, The  $\alpha$ -helix as an electric macro-dipole, *Adv. Biophys.* 9 (1976) 1–63.
- [337] W.G.J. Hol, P.T.V. Duijnen, H.J.C. Berendson, Alpha helix dipole and the properties of proteins, *Nature* 273 (1978) 443–446.
- [338] B. Roux, S. Berneche, W. Im, Ion channels, permeation and electrostatics: insight into the function of KcsA, *Biochemistry* 39 (44) (2000) 13295–13306.
- [339] V.D. Daggett, P.A. Kollman, I.D. Kuntz, Free-energy perturbation calculations of charge interactions with the helix dipole, *Chem. Scr.* 29A (1989) 205–215.
- [340] M. Gilson, B. Honig, The energetics of charge–charge interactions in proteins, *Proteins* 3 (1988) 32–52.
- [341] P.T. Vanduijnen, B.T. Thole, W.G.J. Hol, Role of the active-site helix in Papain, an Abinitio molecular-orbital study, *Biophys. Chem.* 9 (1979) 273–280.
- [342] J. Åqvist, H. Luecke, F.A. Quiocho, A. Warshel, Dipoles localized at helix termini of proteins stabilize charges, *Proc. Natl. Acad. Sci.* 88 (1991) 2026–2030.
- [343] P.J. Lodi, J.R. Knowles, Direct evidence for the exploitation of an alpha-helix in the catalytic mechanism of triosephosphate isomerase, *Biochemistry* 32 (1993) 4338–4343.
- [344] B. Roux, R. MacKinnon, The cavity and pore helices the KcsA K<sup>+</sup> channel: electrostatic stabilization of monovalent cations, *Science* 285 (1999) 100–102.
- [345] F.C. Chatelain, N. Alagem, Q. Xu, R. Pancaroglu, E. Reuveny, D.L. Minor, The pore helix dipole has a minor role in inward rectifier channel function, *Neuron* 47 (2005) 833–843.
- [346] S. Braun-Sand, M. Strajbl, A. Warshel, Studies of proton translocations in biological systems: simulating proton transport in carbonic anhydrase by EVB based models, *Biophys. J.* 87 (2004) 2221–2239.
- [347] S. Braun-Sand, A. Burykin, Z.T. Chu, A. Warshel, Realistic simulations of proton transport along the gramicidin channel: demonstrating the importance of solvation effects, *J. Phys. Chem., B* 109 (2005) 583–592.